ACCELERATED SCIENCE EVALUATION of OZONE FORMATION IN THE HOUSTON-GALVESTON AREA:

Meteorology

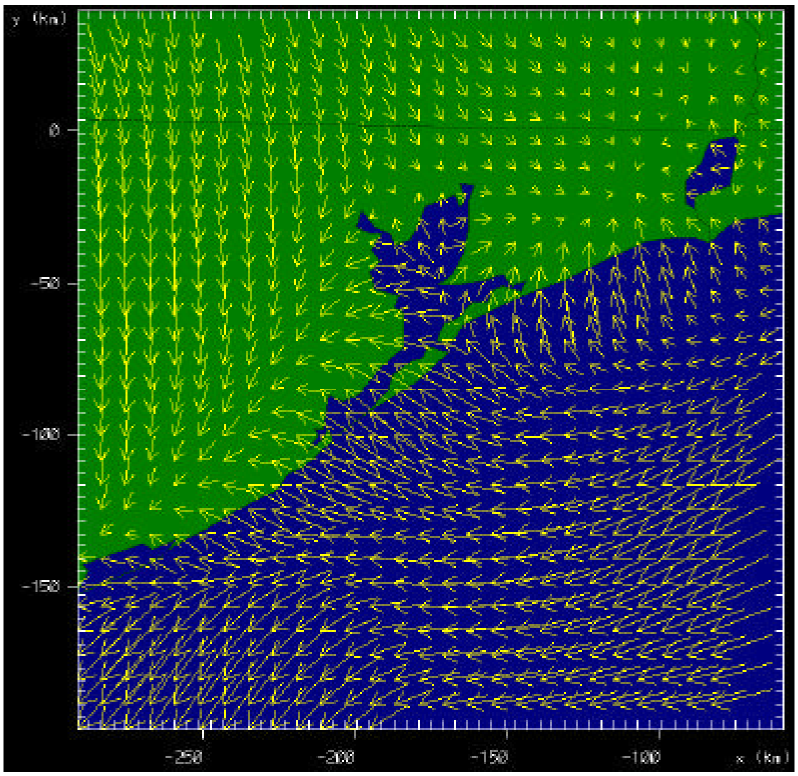

Working Committee
David Allen, University of Texas
Cyril Durrenberger, University of Texas
Gary McGaughey, University of Texas
John Nielsen-Gammon, Texas A&M University
TNRCC Technical Analysis Division

May 30, 2002

Summary

Meteorology plays a critical role in analyzing ozone formation. Data from meteorological models are used in photochemical models to characterize advection, dispersion, temperatures and other critical parameters. These photochemical models, in turn, are used to assess the effectiveness of proposed air quality regulations.

This report focuses on the ability of current meteorological models to predict parameters such as wind speed, wind direction, mixing height, and temperature in the Houston-Galveston (HG) area and the effect of these variables on air pollutant concentrations. The report is organized into the following sections.

First, the meteorological conditions correlated with measured high ozone concentrations in the HG area will be described.

Second, the previous applications of meteorological models in the HG area will be summarized. The spatial and temporal scales used in the models, the procedures used to describe meteorology in these applications, and the results of the performance evaluations will be described.

Finally, key science questions will be described. These questions are partially based on the results of meteorological model simulations using data collected during the Texas Air Quality Study (TexAQS).

The meteorological modeling performed for the TexAQS period suggests that the meteorology affecting the formation, accumulation, and transport of ozone is more complex than previously thought. These findings will be used to revise the conceptual model for formation of high ozone in the HG area.

Further, the preliminary modeling indicates that land surface characteristics (e.g., land use and soil moisture), model vertical grid structure, and the algorithm used for parameterization of the planetary boundary layer (PBL) will be among the more sensitive inputs for meteorological models. In addition, nudging of the modeled winds using measurement data collected from the TexAQS radar wind profilers will be necessary to obtain an acceptable simulation of the three-dimensional wind field. Based on analyses performed to date, an optimal meteorological model (MM5) configuration was selected for the August 25 - September 1, 2000 episode. The MM5 model was run with 42 vertical layers and one-way nesting using the Medium Range Forecast (MRF) PBL scheme. Soil moisture was varied during the episode period to simulate evaporation or precipitation that occurred prior to the episode. The MM5 simulations accurately predict maximum temperatures and reproduce the large-scale temperature patterns. The model performance is good, but relatively less successful in the simulation of minimum temperatures, nocturnal temperature inversions, and the urban heat island. Observational nudging of the winds using the TexAQS radar wind profiler data provided an improved

simulation of the tropospheric winds; however, there remains a systematic underestimate of the strength of the sea breeze inversion. This could lead to unrealistically large diffusion of constituents into and out of the advancing marine air. In addition, the MM5 model does not predict the strength and vertical structure of the nocturnal low-level jet that occurred on some days, suggesting that the current results will overestimate the amount of nighttime vertical mixing.

Contents

Background

Structure of the report

Meteorological conditions correlated with high ozone in the HG area

Application of meteorological models in the HG area

Model Performance Evaluation

Key scientific questions

1. What meteorological conditions are associated with high ozone concentrations in the Houston Galveston area during the Texas Air Quality Study?

2. What atmospheric processes lead to the conditions conducive to ozone formation?

3. Can available meteorological models adequately simulate these processes?

4. How can observations best be assimilated into a meteorological model to enhance its representation of these processes?

5. What is the minimum set of routine observations needed to adequately simulate the meteorological parameters used for photochemical grid modeling?

6. Are linkages between meteorological and photochemical grid models accurately transferring wind field information?

Background

The HG area currently violates the National Air Quality Standard for ozone, and has been classified as a severe nonattainment area under the Federal Clean Air Act Amendments for 1990 (FCAA, 1990). For areas that are designated severe, the 1990 FCAA requires that photochemical grid models be used to assess the air quality benefits of emission reductions included in state implementation plans (SIP). Photochemical grid models use meteorological data and emissions data to predict ozone concentrations and the sensitivity of ozone concentrations to emissions reductions. A multi-day time period (called an episode) that is representative of the conditions that are correlated with high ozone concentrations is used as the basis of the photochemical grid modeling.

Meteorological models provide critical inputs to photochemical models. In general, meteorological models use a set of measurements taken at limited times and at a limited number of sites, along with models of physical processes, to predict the physical behavior of the atmosphere. For example, for historical episodes in the 8-county HG ozone nonattainment area, inputs to the meteorological model include hourly surface observations of wind speed, wind direction, temperature, and solar insolation that are measured at approximately 25 (the exact number varies from year to year) continuous monitoring sites. Hourly National Weather Service (NWS) observations collected at several Houston area airports are also used, as are marine observations from several buoys and coastal platforms. When available, vertical measurements of wind speed, wind direction, and temperature obtained from twice-daily vertical rawinsonde soundings and/or continuous data from sodar sounders and radar profilers are utilized. Larger-scale gridded analyses and meteorological model forecasts from agencies such as the National Centers for Environmental Prediction (NCEP) that incorporate regional and global scale observations from a variety of platforms are included as well. In addition, meteorological models may also require inputs such as surface roughness and land use data on a grid-point basis.

Using these input data to predict three dimensional wind speed, wind direction and other parameters at all times of the day and over the entire HG area is complex. With no significant topography to trap pollutants, large-scale and local-scale winds must combine to produce temporarily stagnant conditions or shallow mixing depths. During periods of weak to moderate large-scale winds, which are favorable for high ozone concentrations, the winds over southeast Texas are dominated by the land-sea breeze circulation. Observations of the land-sea breeze demonstrate a circular (clockwise) rotation of the near-surface winds. This diurnal oscillation likely contributes to the recirculation of air parcels over the HG area on some days. Near the coastline, a sea breeze front can develop, with light winds ahead of the front and a shallow mixed layer beneath the front. The inland penetration of the sea breeze front varies from day-to-day depending upon the speed and direction of the large-scale wind and strength of the diurnal land-sea temperature gradient. The spatial variability of surface temperatures over land, including the effects of the urban heat island, further modulate the winds. In addition, the near-surface flow is sometimes complicated by strong vertical shear in the lowest few hundred meters of the atmosphere, often indicating the presence of a low level jet. These complexities tax any meteorological model to accurately simulate the winds at the surface and in the vertical.

In addition to the need for detailed meteorological data with fine scale spatial and temporal resolution for air quality modeling, meteorological data are also required for the identification of meteorological processes that lead to ozone formation and the selection of appropriate episodes to be modeled. The process of using meteorological data and models to identify conditions that lead to the formation of ozone is referred to as conceptual model development. These uses of meteorological data are shown in Figure 1.

Figure 1.

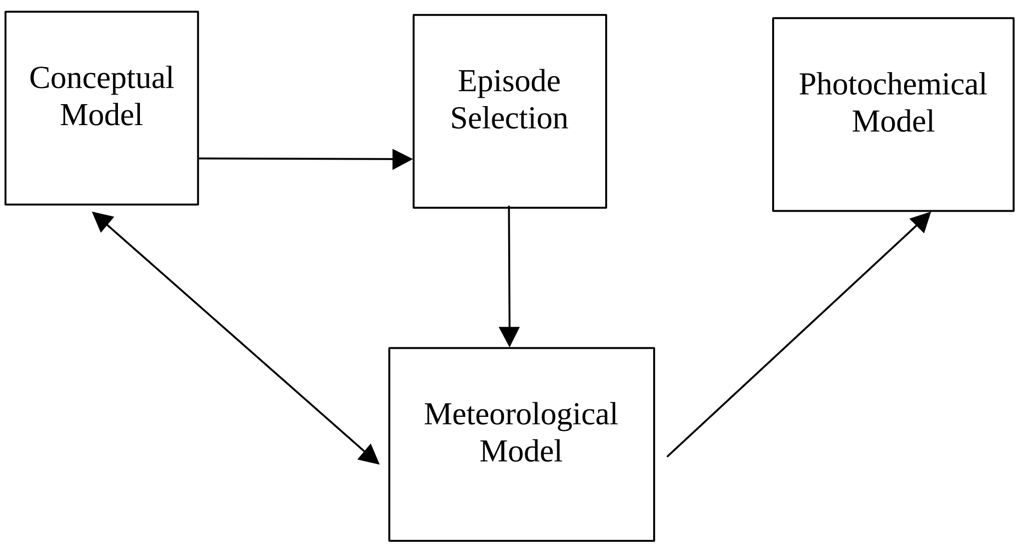

Structure of the report

The focus of this report is on the ability of current meteorological models to predict the magnitude, spatial distribution and temporal distribution of critical meteorological parameters related to ozone formation in the Houston Galveston (HG) area. To address this issue, the report will be organized into a number of sections.

First, the meteorological conditions correlated with measured high ozone concentrations in the HG area will be described.

Second, the previous applications of meteorological models in the HG area will be summarized. The spatial and temporal scales used in the models, the procedures used to describe meteorology in these applications, and the results of performance evaluations will be described.

Finally, key science questions will be described.

This report will build on other reports developed in the Accelerated Science Evaluation of ozone formation in the Houston-Galveston Area and interested readers can obtain these reports at www.utexas.edu/research/ceer/texaqsarchive.

Meteorological Conditions Correlated with High Ozone in the HG area

The TNRCC has developed a conceptual model of ozone formation in the HG area (TNRCC, 2001). The conceptual model provides an analysis of the correlations between observations of high ozone concentrations and meteorological parameters. Key features of the conceptual model are summarized below. More details are available in the full report (TNRCC, 2001).

Temporal Analysis

Days characterized by high ozone concentrations have been observed in the HG area in almost every month, but the greatest frequency of high ozone concentrations occurs during late August and early September. An analysis of the days of the week characterized by high ozone concentrations shows that there is no clear difference between week days and weekend days. The diurnal pattern of high ozone concentrations shows that monitoring stations frequently measure distinct high peaks of ozone for only one or two hours. During times when high ozone concentrations are measured at a number of sites, the high ozone concentrations are observed at different hours at different sites, with a tendency for the high ozone concentrations to move downwind with time. On many days, pulses of high ozone concentrations “appear to form in eastern Harris county and then traverse across the HG domain, where they are observed briefly as they pass each monitoring site” (TNRCC, 2001). Figure 2 (TNRCC, 2001) shows the average time of day of the peak ozone concentration at monitoring stations in the HG area. On average, the earliest times for peak ozone concentrations occur in the Deer Park/La Porte area at approximately noon. The average time of the peak ozone concentrations becomes later as one moves farther north from the Deer Park/La Porte area.

Figure 2. Average time of the peak ozone concentration in the HG area. Times reported on a 24-hour basis in blue. (TNRCC, 2001)

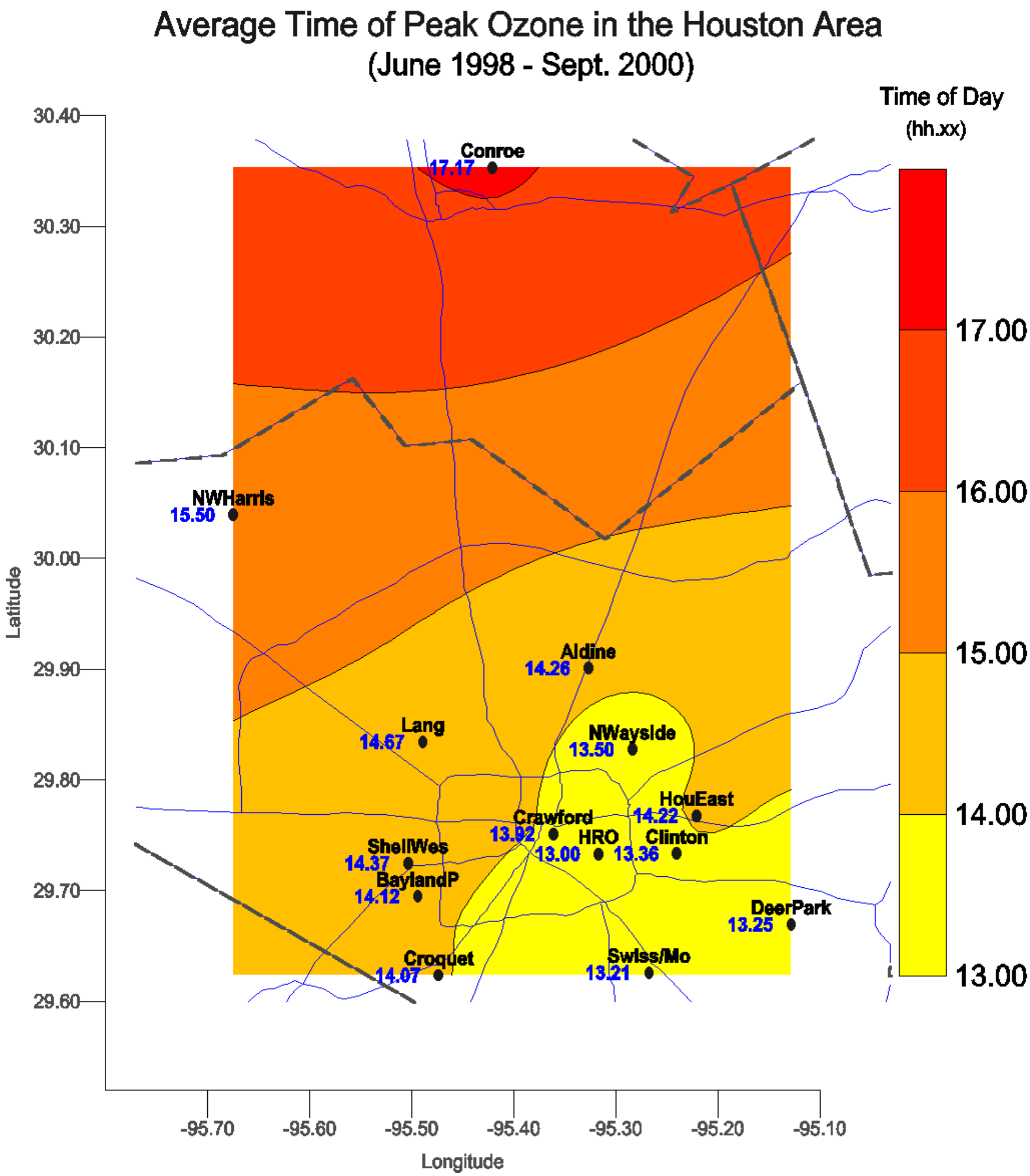

Spatial Analysis

TNRCC analyzed the number of days at each monitoring station characterized by a 1-hour ozone concentration that exceeded the 1-hour standard. There are three areas with the highest frequency of exceedance days – near Deer Park in the east, near Croquet/Bayland Park in the west and near Aldine in the north. Figure 3 (TNRCC, 2001) shows the number of exceedance days for the period from 1998 to 2000.

Figure 3. HG area expected exeedance days 1998-2000. Sites with fewer than three years of data were normalized to be equivalent to three years of data. (TNRCC, 2001)

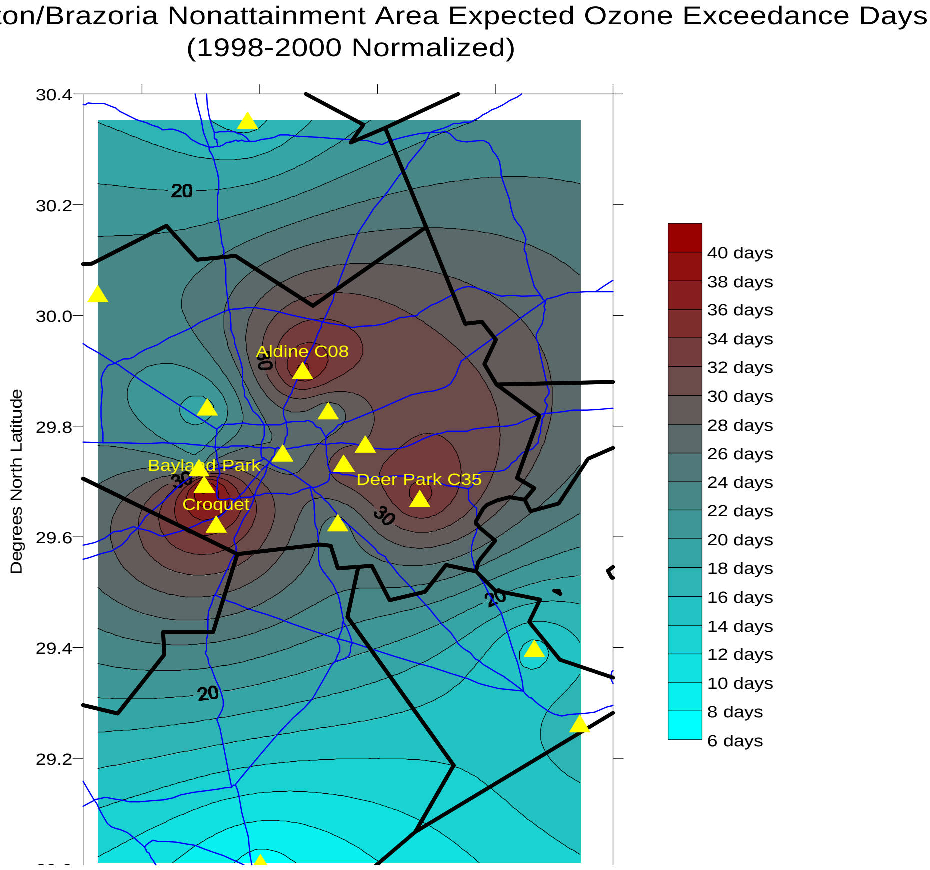

The design value at a monitoring site is defined as the fourth highest daily one-hour value measured over a continuous three-year period at that site. The design value for an area is the highest design value over all of the monitoring sites in the area. Figure 4 (TNRCC,

2001) shows a map of the design values in the HG area for 1998 to 2000. The maximum value was 199 ppb at the Clinton monitoring site. The location of the design value moves from year to year, but generally remains in the eastern part of the city.

Figure 4. HG ozone design values 1998-2000. (TNRCC, 2001)

Houston/Galveston/Brazoria Area Ozone Design Values 1998-2000

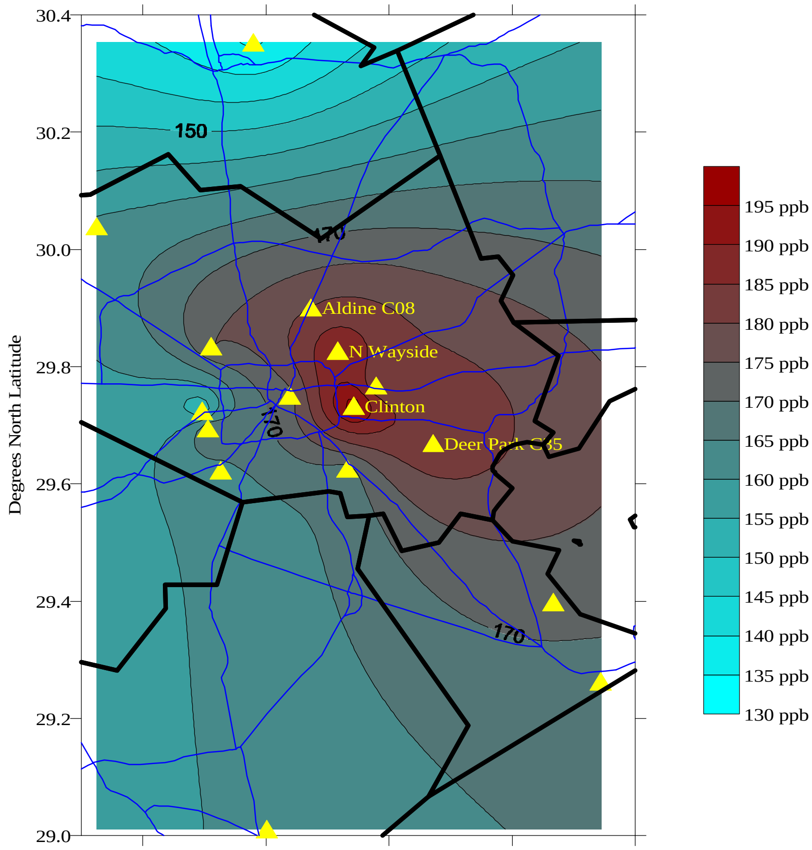

Wind Pattern Analysis

During the summer, high pressure typically persists over the Gulf of Mexico, often leading to stagnant conditions and weak pressure gradients in southeast Texas. This weak synoptic scale forcing allows local influences to dominate the weather patterns. In the HG area there are persistent sea breezes along the coastline, bay breezes near Galveston Bay, land-sea breeze flow reversals, and a shoreline convergence zone that may move inland. Away from the coast, the winds in southeast Texas undergo a regular daily clockwise rotation, with the strongest onshore flow in the early evening, although this wind pattern is suppressed when winds are strong.

EPA guidance for photochemical modeling (EPA, 1991) recommends selecting photochemical modeling episodes using analysis of morning winds during high ozone events. However, since the role of flow reversals in southeast Texas has been recognized for some time, the Texas Air Control Board (TACB) enhanced this process by adding an analysis of afternoon winds. More recent analyses (TNRCC, 2001) indicate that a 24-hour analysis is more appropriate. These recent results indicate that on high ozone days, the wind direction rotates continuously during a 24-hour period. Average winds blow from the southwest around midnight, then gradually shift to northwest and northeast during the morning hours. By noon the average winds are from the east, followed by southeasterly flow in the early afternoon. After sunset the winds shift to the south and west and the pattern may repeat the next day. This pattern is shown in Figure 5 (TNRCC, 2001).

Figure 5. Average wind circulation pattern on days when high ozone is measured in the HG area. Each blue diamond on the diagram represents the starting point of a wind vector that ends at the origin. The diamonds representing midnight and noon conditions are labeled. The 24-hour average, net wind vector is show in red.

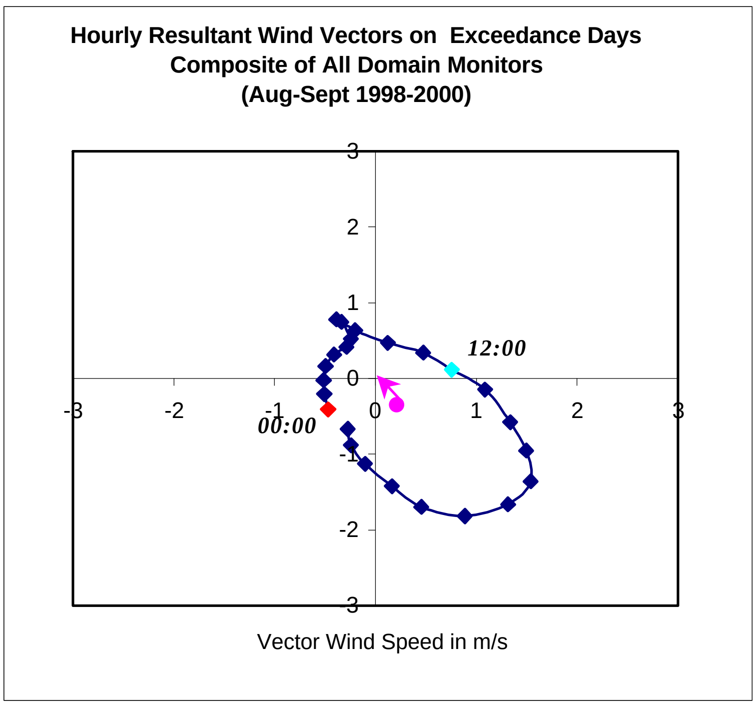

On days with low measured ozone, the 24-hour winds show a much different pattern. The westerly, northwesterly and northeasterly components are not present and the prevailing wind direction is, on average, from the east to southeast. There is normally a persistent sea breeze from the southeast that results in ventilation and transport of pollutants downwind rather than concentration and recirculation of pollutants. This pattern is shown in Figure 6 (TNRCC, 2001).

Figure 6. Wind circulation pattern on days when low ozone is measured in the HG area (TNRCC, 2001). The nomenclature is the same as used in Figure 5.

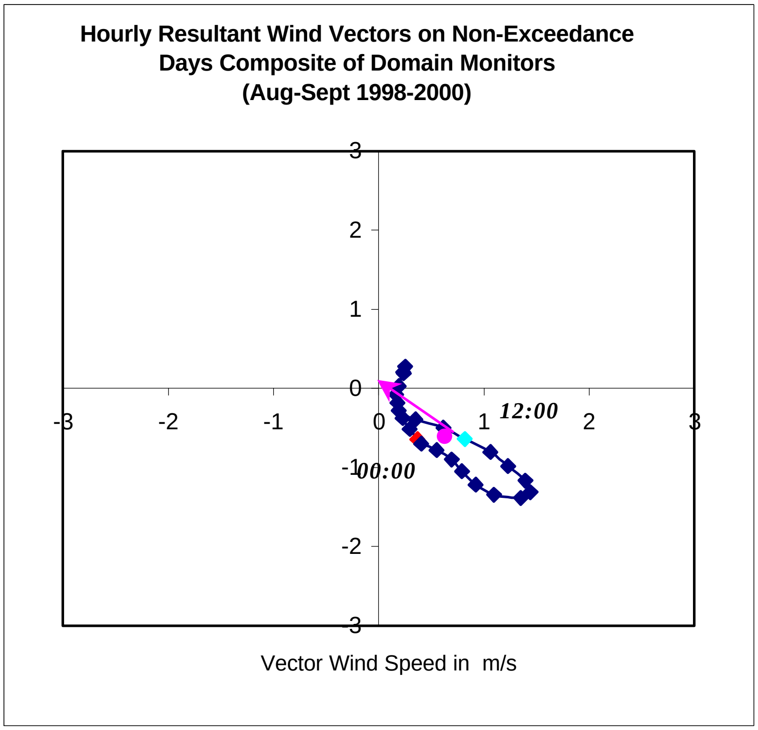

Trajectory Analysis

Air parcel trajectories using surface measurements of wind direction and wind speed have been used to estimate the path over which an air parcel traveled for a given time period. There are significant uncertainties associated with these trajectory analyses on some days. Surface winds measured at a limited number of sites do not necessarily represent wind fields aloft, and may be spatially representative for only the local area. This will be particularly true during atmospheric conditions characterized by a wind speed and direction that changes rapidly with height above the surface, conditions sometimes observed during the nighttime hours in the HG area.

Surface trajectories have been analyzed for days when high ozone concentrations were measured and compared to those when low ozone concentrations were measured. On days characterized by high ozone, the trajectories typically show the change of wind direction and the flow reversal shown in Figure 5. The average trajectory associated with this pattern is shown in Figure 7 (TNRCC, 2001).   Figure 8 presents the trajectory shown in Figure 7 on a map of the HG area. The red diamond represents the location of the air parcel at midnight when the trajectory was initiated. The dark blue diamonds represent the location of the air parcel at each subsequent hour of the day. The trajectory indicates that the air parcel moves to the southeast toward Galveston Bay during the early morning hours. The wind direction shifts to the east and southeast by noon, carrying the parcel to the northwest. Later in the afternoon, southerly winds move the air parcel northward.

Figure 2 shows that the average time when the peak ozone concentration is measured becomes later in the day as one moves north of the city. Figures 2 and 8 suggest that a pool of high ozone forms in the morning hours and is advected to the northwest and northeast during the afternoon. In contrast, days characterized by low ozone concentrations are not characterized by this flow reversal and the trajectory indicates movement of the air parcel to the northwest throughout the day, as shown in Figure 9 (TNRCC, 2001).

Figure 7. Average surface trajectory on days when high ozone is measured in the HG area (TNRCC, 2001). The trajectory begins at the origin at midnight. Hourly average wind directions and wind speed are then integrated (added head to tail) to estimate a trajectory.

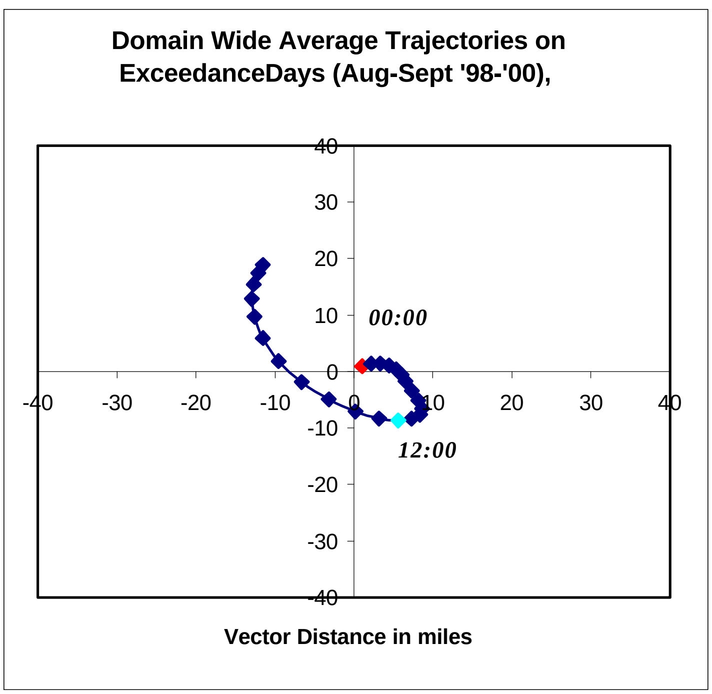

diamonds represent the location of the air parcel at one-hour intervals. The red diamond represents the initiation of the trajectory at midnight. The dark blue diamonds show the

local time. The second light blue diamond shows the location of the air parcel at 12:00 noon.

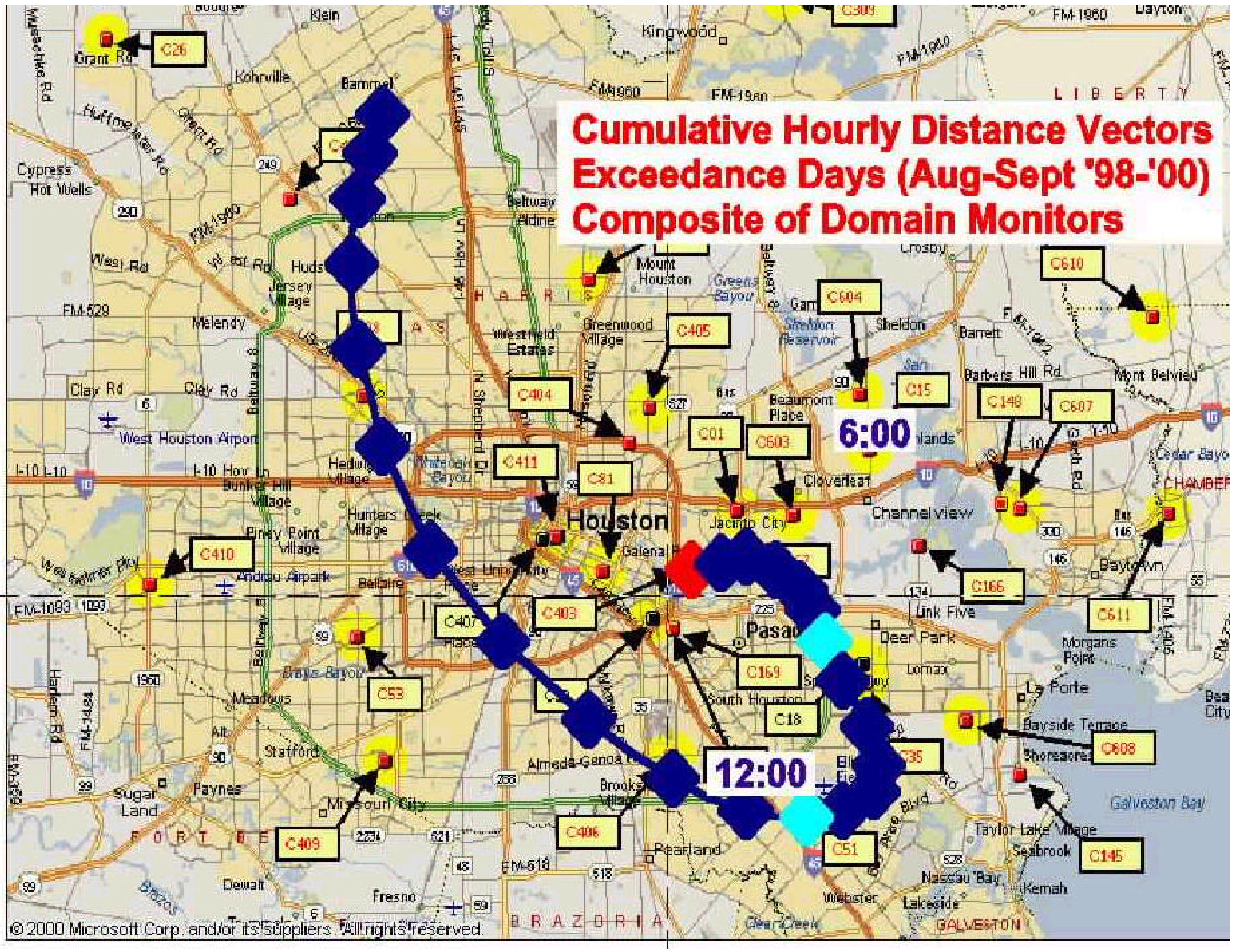

Figure 9. Average surface trajectory on days when low ozone is measured in the HG area (TNRCC, 2001). The trajectory begins at the origin at midnight. Hourly average wind directions and wind speed are then integrated (added head to tail) to estimate a trajectory.

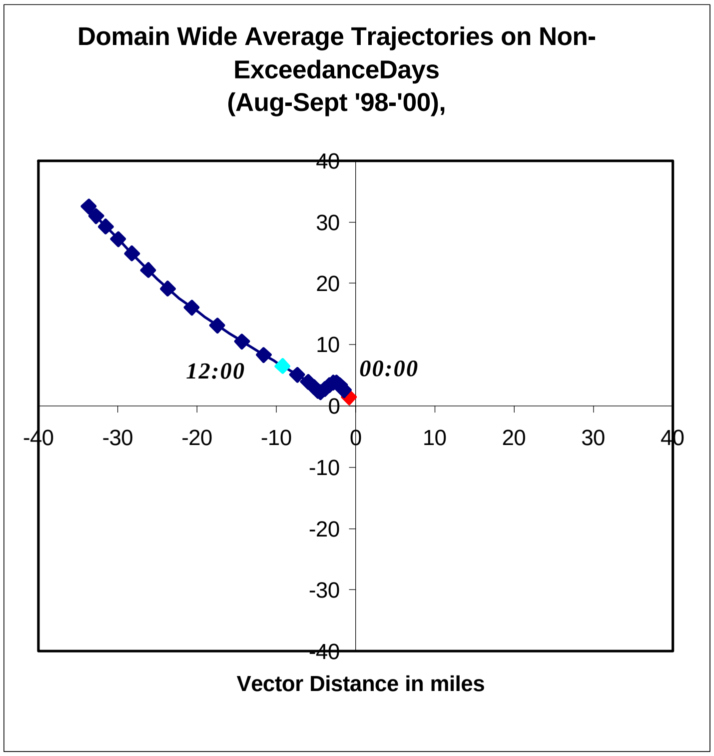

The movement of air masses by upper level winds can result in significant regional transport of pollutants. The NOAA HYSPLIT tool (www.arl.noaa.gov/ss/models/hysplit) has been used to characterize this transport. The trajectory calculations are based on archived model forecast data developed for very large grid cells (80 to 108 km) at a temporal resolution of three-hours. The relatively low spatial and temporal resolution probably captures the prevailing synoptic flow during weather patterns dominated by large-scale and slow-moving systems. HYSPLIT trajectories initialized at 500 meters above the surface were analyzed on all days characterized by high ozone concentrations in HG area during 1995 and 1996. These trajectories indicated long-range transport of air into Southeast Texas from all directions with the exception of the west and northwest. Multi-day trajectories suggested that long-range transport of pollutant emissions from sources located from the central and eastern U.S. may have occurred on some days. Of course, regional transport of pollutants out of the HG area occurs as well. Regional modeling performed by The University of Texas for three historic episodes also indicated that ozone from the HG area contributed to high ozone in other areas and that ozone was transported into the HG areas from several directions. (McDonald-Buller, 2000). The transport directions sometimes vary greatly with height above the surface, particularly during the nighttime hours when the wind speed and direction show significant variation with height. This has been recently illustrated by calculating trajectories based on wind data collected at a TexAQS radar wind profiler, as shown in Figure 10 (Senff, 2001).

Figure 10. 12-hour forward trajectories for four altitudes for August 29, 2000. (Senff, 2001)

Forward Trajectories for the Night of 8/29

Start: 8/29 18:00 CST   End: 8/30 06:00 CST

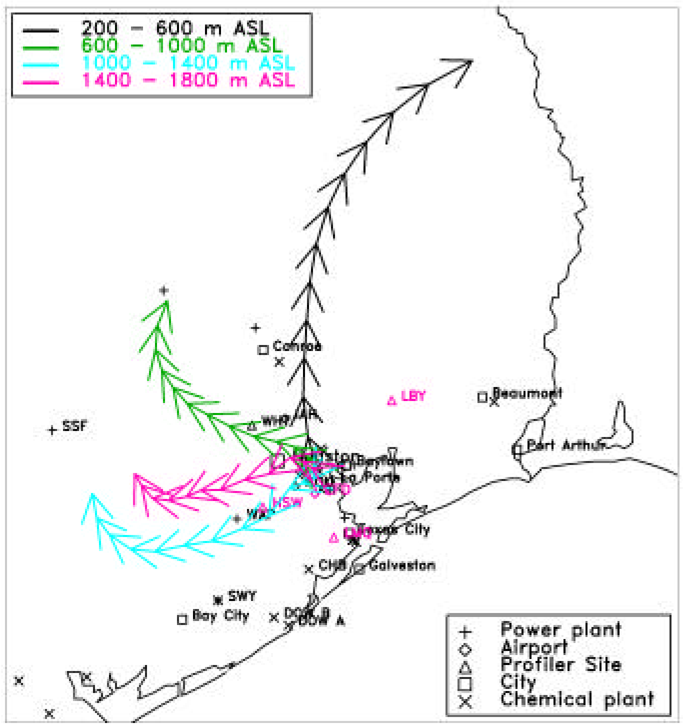

Summary of conceptual model

In general the conditions most often correlated with the highest ozone levels in the HG area are:

- light large-scale winds,
- warm temperatures,
- Ozone precursors accumulate (concentrate) during the night as a result of low wind speeds and low mixing levels,
- Light winds move the concentrated pool of precursors to the southeast in the morning,
- Ozone concentrations build in the presence of sunlight in the morning,
- Winds move the pool of ozone to the west and northwest, and
- Flow reversal carries the pool of ozone back over the city.

Application of meteorological models in the HG area

As described in detail in the Accelerated Science report on Air Quality Modeling, the TNRCC has used photochemical grid models to develop air quality management plans (state implementation plans) in 1994, 1998, 1999 and 2000. Each of these photochemical modeling applications has involved meteorological modeling. The meteorological modeling used to support these photochemical grid modeling applications will be briefly described below.

Meteorological models consist of mathematical equations that describe how atmospheric temperature, pressure, and moisture change with time. To run a meteorological model, a fixed three-dimensional grid is defined over the domain to be modeled and all of the physical processes are accounted for in each grid cell. Typically, several sizes of grids are nested together. Figure 11 presents the vertical coordinate system used by the MM5 model. The sigma coordinate system is defined as the ratio of pressure at a given level above the surface divided by the surface pressure. Sigma surfaces near the ground are terrain following while upper sigma surfaces are flat. The MM5 model predicts pressure perturbation, east-west (u) and north-south (v) components of the horizontal wind, temperature, and water vapor at half sigma levels; vertical velocity is calculated at full sigma levels. Additional meteorological quantities of interest (e.g., relative humidity, mixing heights) are calculated from these variables. The quantities derived from the meteorological model that are required by the photochemical model are, in order of importance: wind speed, wind direction, mixing height, temperature, and specific humidity.

Figure 11. Schematic representation of the vertical coordinate system of the MM5 model. The example is for 15 layers. Dashed lines denote half-sigma levels, solid lines denote full-sigma levels. Figure was obtained from *Tutorial Class Notes and User's Guide: MM5 Modeling System Version 3* (January 2001)

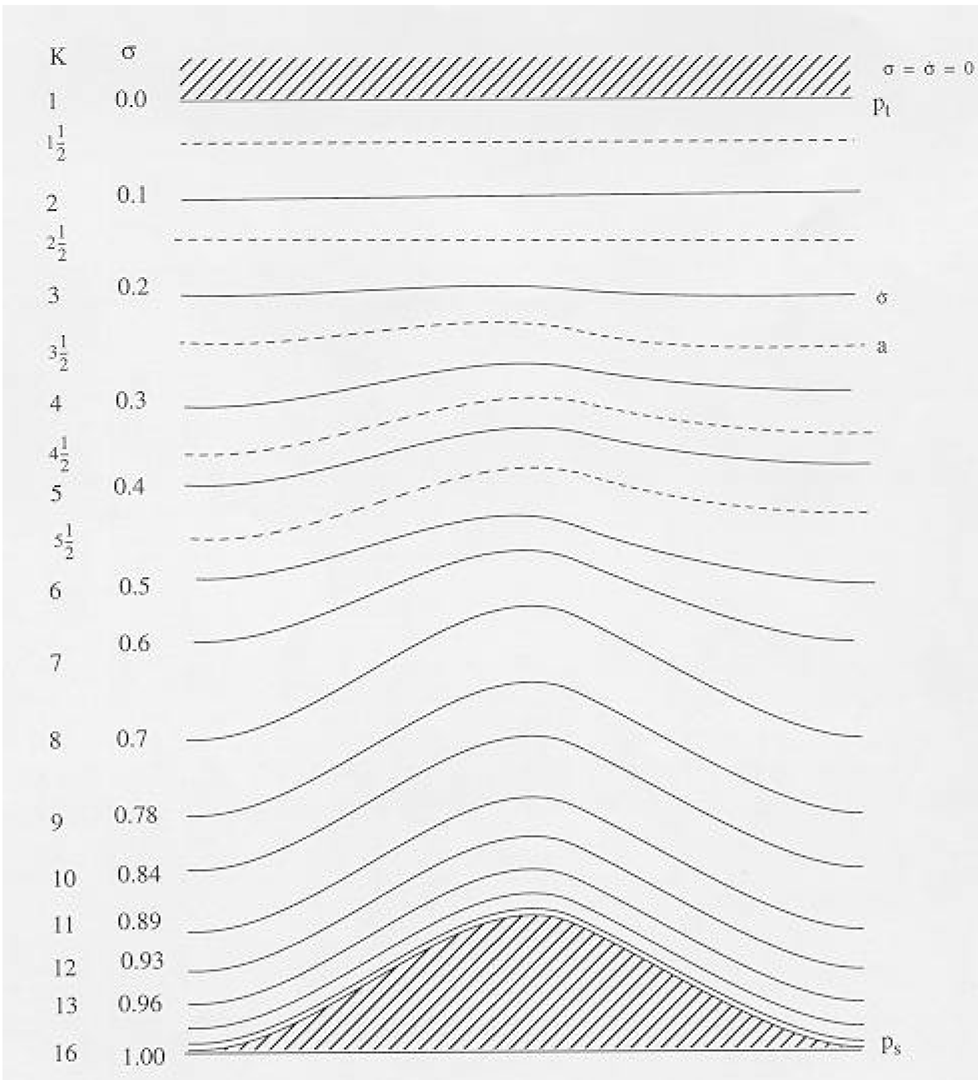

To run properly, the meteorological model should be run over a domain that is much larger (on the order of 100's of km) than the domain selected for photochemical grid modeling. Typically photochemical grid models use a horizontal grid spacing of 4 km for the urban area being modeled. Within each grid cell, the atmosphere is assumed to be uniformly (well) mixed. Wind speeds, wind directions, temperatures and other parameters are assumed to vary smoothly within the grid cell. As smaller and smaller grid cells are used, more details of the atmosphere become resolvable by the model; however, use of small grid cells may make the parameterizations of physical processes used in the model inaccurate. Achieving an appropriate balance between the accuracy of the model's assumptions concerning mixing and the data demands imposed by the model is one of the most difficult challenges in formulating meteorological models. In most regions, when using MM5, grid cells of 1-4 kilometers in horizontal dimension and 20 – 500 meters in vertical dimension are the smallest considered implementable. Placing a 4 km horizontal grid structure over the whole domain needed for the meteorological model is unnecessary for photochemical modeling and would require an extremely large amount of storage space and computational time. To get around this problem, meteorological models have been designed to use various sized grids that are nested, with the horizontal size increasing as one moves away from the urban domain.

Photochemical grid models use the same approach for a grid structure as used by meteorological models, but add emissions and chemical processes to a few of the physical processes simulated with the meteorological model. Photochemical models are frequently run with fewer vertical layers than used with meteorological models. The number of vertical layers in photochemical models is typically chosen to adequately resolve the vertical variations in pollutant concentrations that affect pollutant concentrations near the ground. Meteorological models require a relatively greater number of vertical layers since processes throughout the depth of the atmosphere impact the near-surface meteorology. For example, for the modeling with the August 25 - September 1, 2000 episode, the meteorological model is being run with 42 vertical layers that extend to a height of approximately 20 km above the surface while the photochemical model is being run with 11 vertical layers that extend to a height of approximately 3 km above the surface. Normally for photochemical models the vertical layers near the surface are selected to be identical to the layers used in the meteorological model.

CSUMM

In 1988 the TACB purchased the Urban Airshed Model version IV (UAM-IV) and had its staff trained to use the model. At that time the UAM-IV was the state-of-the-science photochemical grid model and was listed by EPA in the "Guidelines on Air Quality Modeling" (EPA, 1986) as a preferred air quality model for ozone modeling. The TACB had a consultant use a prognostic meteorological model and the UAM-IV to model the HG area with a set of historical data.

The Colorado State University Mesoscale Model (CSUMM)(Kessler, 1989) prognostic hydrostatic, meteorological model was used to develop the meteorological inputs for the UAM-IV model. CSUMM is based on atmospheric primitive equations that are simplified by the hydrostatic, incompressible Boussinesq approximations. It includes a surface heat budget and detailed parameterizations of the atmospheric surface and planetary boundary layers (PBL). A terrain following system is used. The following information is required to run the model:

- Topography
- Land/water coverage
- Domain-scale initial profiles for potential temperature and specific humidity
- Domain-scale geostrophic winds

The model generates the following fields for each grid cell and each reporting time interval (usually one hour) of the simulation:

- Horizontal wind components
- Vertical wind component
- Potential temperature
- Specific humidity
- Gridded field of planetary boundary layer heights (related to mixing height)

Further details of the model may be found in Mahrer and Pielke (1977, 1978) and in Arritt (1985).

The grid cells used for the CSUMM and UAM-IV were 5 km x 5 km over a domain that covered the HG and Beaumont/Port Arthur areas as shown in Figure 12. The CSUMM modeling used 19 layers in the vertical while the UAM-IV modeling used 5 layers in the vertical. The UAM-IV has vertical layers that change hourly in height based on the hourly rise and fall of the mixed layer. Two vertical cells were located below the mixing height and three were located above the mixing height.

Performance evaluation of CSUMM results is covered in detail in the 1994 SIP (TNRCC, 1994). These evaluations were graphical in nature and compared hourly modeled values to measured values for wind direction and wind speed at selected monitoring sites.

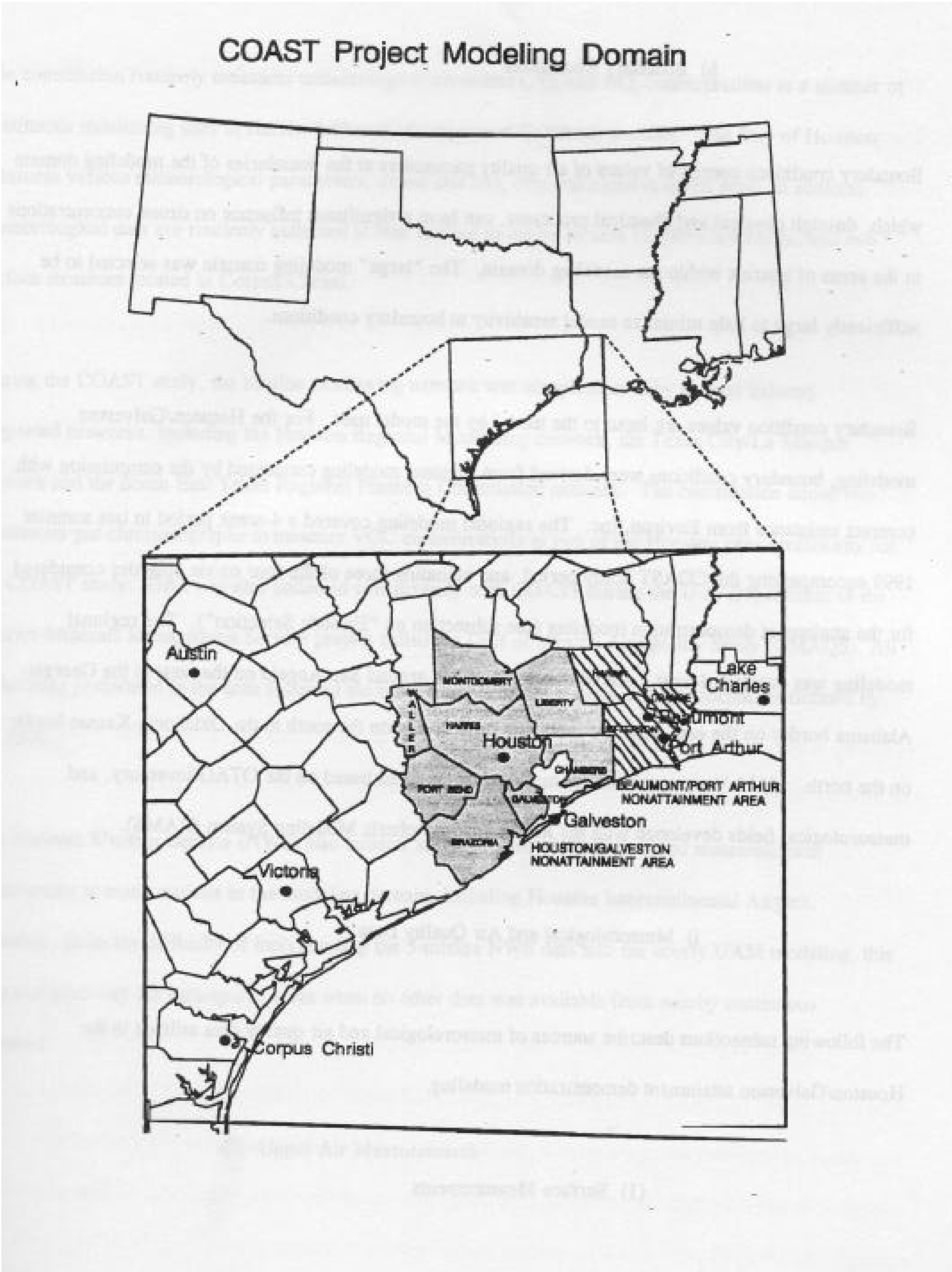

Figure 12. Coast Modeling Domain

SAIMM

One of the recommendations to emerge out of the UAM-IV photochemical grid modeling and supporting meteorological modeling was that a detailed field program be performed to collect meteorological and air quality data. As a consequence, the Coastal Oxidant Assessment for Southeast Texas (COAST) was conducted in July and August 1993 (MMS, 1995). During this period the number of surface monitoring sites continuously measuring ozone and meteorological parameters was increased. Radar profilers and acoustic sounders were installed to measure meteorological parameters in the upper air. On selected days airborne sampling was conducted. These measurements formed a robust data set that was used by TNRCC to provide inputs to run meteorological and photochemical grid models and evaluate their performance.

To utilize the robust COAST data set, a variable grid version (UAM-V) of the UAM was developed. This was an enhanced photochemical grid model that had a number of new approaches. Those relating to meteorological parameters are:

1. The grid structure for vertical cells was fixed in space and time.
2. The model could be run with nested horizontal grid cells of various sizes. In particular it was possible to run the model over part of the domain with a coarse grid of 16 km x 16 km, another part with a medium grid of 4 km x 4 km and a fine grid of 2 km x 2 km.

.

The Systems Applications International Meteorological Model (SAIMM)(Kessler, 1993) was used to develop the meteorological parameters for UAM-V. SAIMM is a hydrostatic prognostic meteorological model, which is an enhancement of the CSUMM described above. The wind fields produced by SAIMM did not initially compare favorably with observed wind fields (TNRCC, 1994) so observations were incorporated into the model continuously with a common four-dimensional data assimilation (FDDA) technique (TNRCC, 1994).

Two sets of model runs were performed with SAIMM and UAM-V. To set boundary conditions for the urban scale modeling domain, regional scale modeling was conducted over a large domain with a horizontal grid of 16 km x 16 km. This domain is shown in Figure 13. The domain for the smaller urban scale modeling is shown in Figure 14. The horizontal grids used for the meteorological model were identical to those used for the regional scale and 4 km urban scale photochemical grid models. For the 2 km photochemical grid modeling, meteorological data were interpolated from the values from the 4 km grid.

Figure 13. Regional Modeling Domain for TNRCC Modeling with the COAST Data

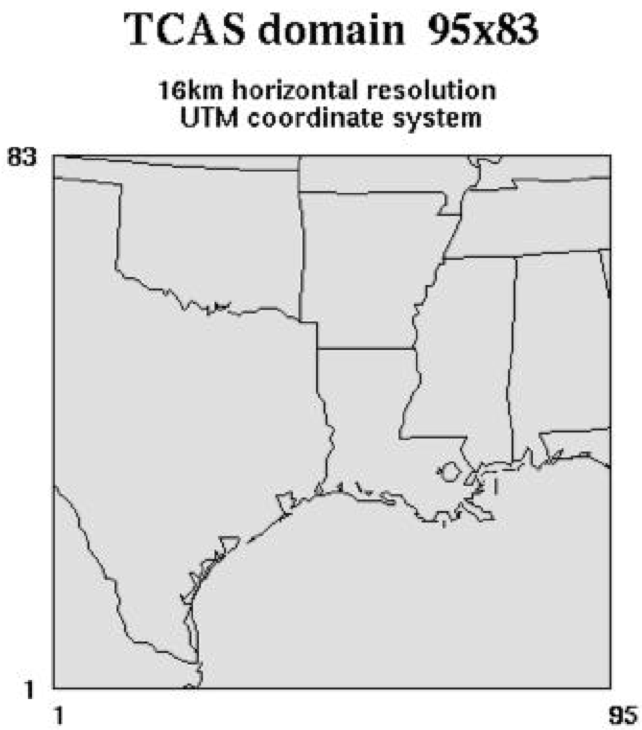

Figure 14. Urban Scale Modeling domain for TNRCC Modeling with the COAST Data

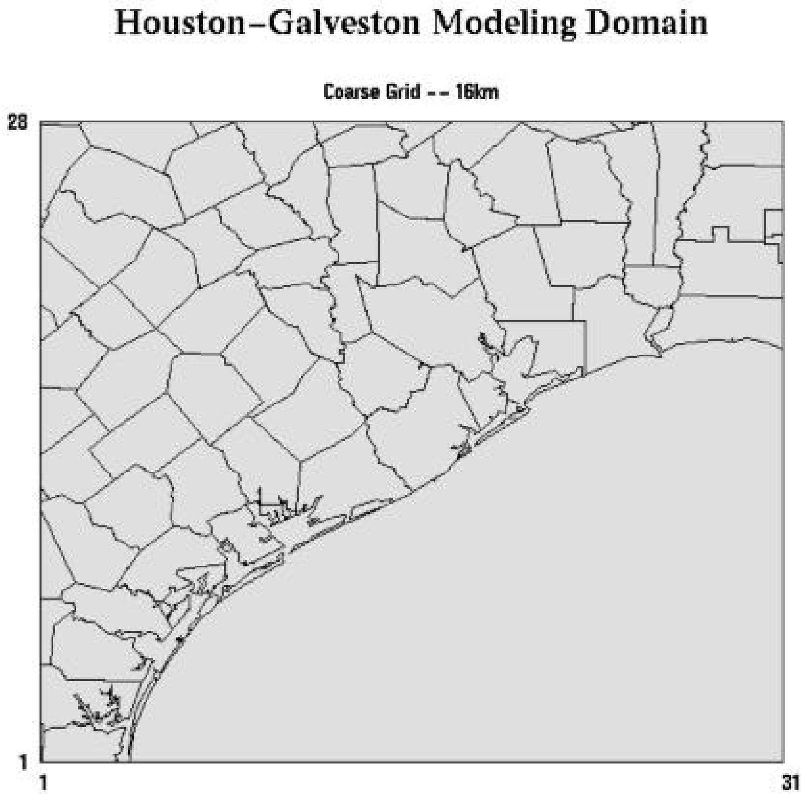

Figure 15 shows the grid cell sizes used in the urban modeling domain that was used for UAM-V modeling. A large 16 km x 16 km grid covered the whole modeling domain. A 4 km x 4 km grid covered both the HG and BPA areas. Two 2 km x 2 km sub domains covered each of the HG and BPA nonattainment areas used in the photochemical grid modeling. A 4 km x 4 km grid covered the Victoria/Corpus Christi areas. Results from the regional modeling were used to define the initial conditions and boundary conditions for the urban scale modeling domain.

Figure 15. Subgrids Used for COAST UAM-V Modeling.

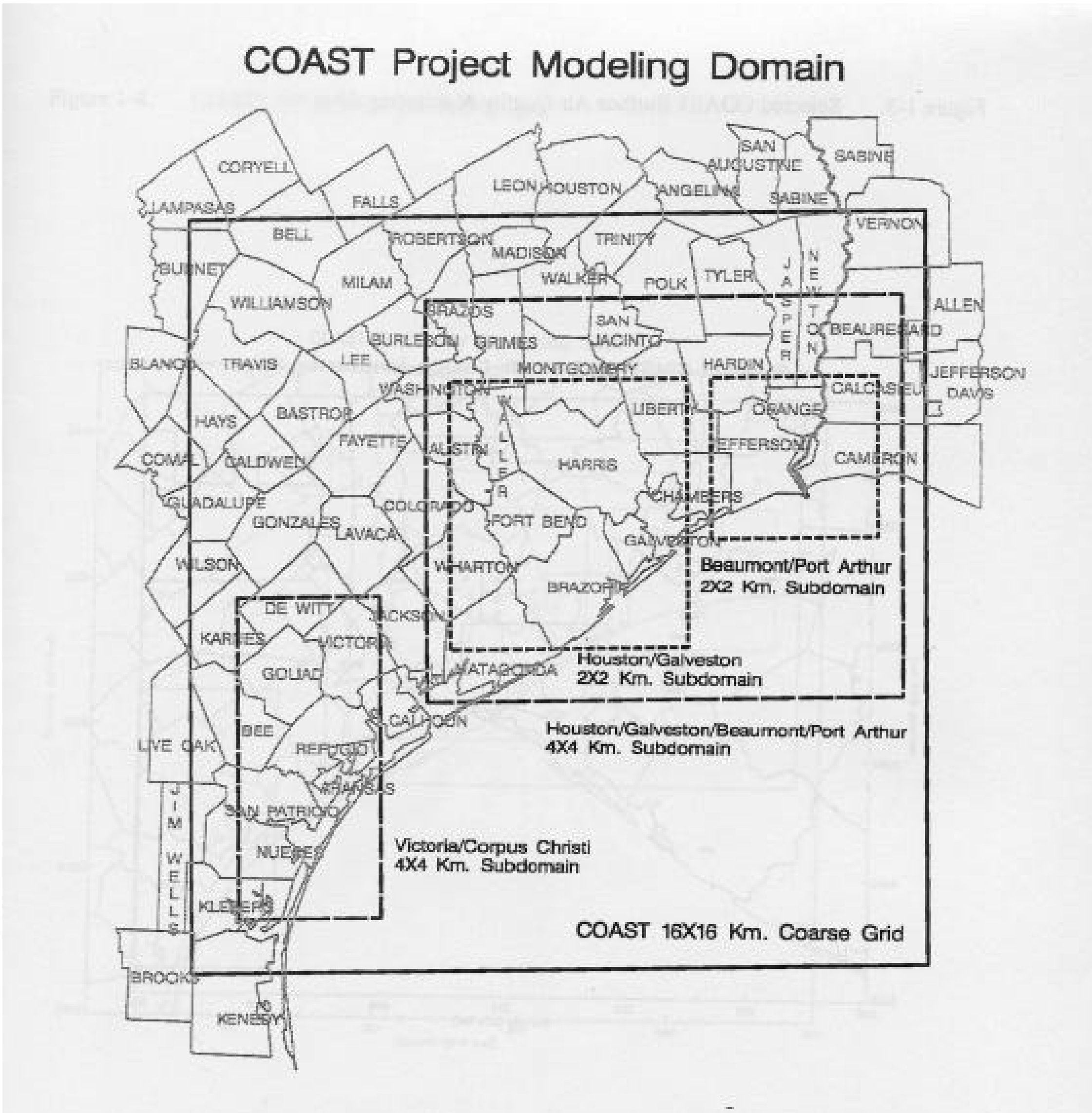

Following EPA guidance (EPA, 1991) four episodes were selected for base case development. These were October 24-25, 1992; August 18-20, 1993; September 1-2, 1993; and September 8-11, 1993.

Initial base case development was performed for each of the four episodes. The October 1992 and August 1993 episodes did not meet performance criteria. After extensive examination and hundreds of sensitivity runs, these episodes were set aside. The September 1-2, 1993 episode, developed for the BPA area, met performance criteria. After additional analyses and emissions inventory enhancements the performance for the September 8-11, 1993 episode met the criteria. Initial sensitivity modeling indicated that it was not necessary to use the extra time and resources to model with the 2 km x 2 km grids, so almost all urban scale modeling was performed with a 4 km x 4 km grid spacing.

Results of modeling for the September 8-11, 1993 episode were used for the HG SIP submitted in 1998 (TNRCC, 1998). After the 1998 SIP was completed TNRCC began using version 1 of Comprehensive Air Quality Model with Extensions (CAMx)(CAMx, 2001) for photochemical modeling. The meteorological parameters were the same as those used for the UAM-V modeling.

With the nesting capability of CAMx, TNRCC moved from running two sets of models, regional and urban, to one model with a nested grid over the regional domain as shown in Figure 16. This has been denoted as the SuperCOAST domain.

Figure 16. SuperCOAST modeling domain with grids used for photochemical modeling with CAMx.

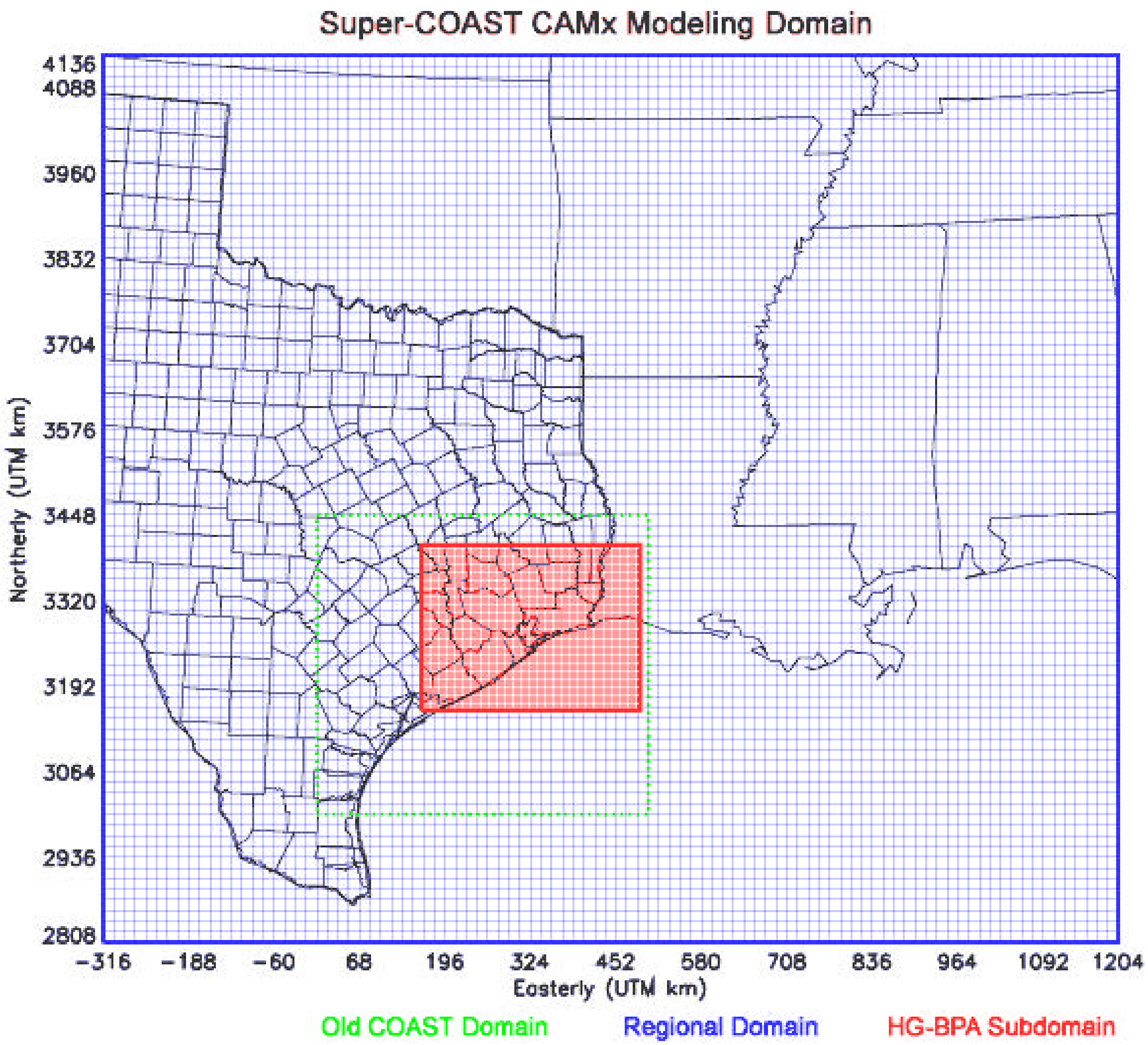

Model Performance Evaluation

The process of comparing model predictions to ambient observations taken at the same time and location is referred to as performance evaluation. The comparisons reveal whether current data and models for processes are accurate representations of the region being modeled. There are two types of model performance evaluation applied to meteorological model results. One type of meteorological model performance evaluation is a comparison of the meteorological model results with meteorological measurements. In the past this has been mainly qualitative in nature, but as described below, a statistical approach has recently been developed. The second type of performance evaluation is based on results from the photochemical grid model. Photochemical grid model performance evaluation is covered in EPA guidance for running photochemical grid models (EPA, 1991). Photochemical grid model performance activities include diagnostic analyses, which evaluate model response based on changes to model inputs. Part of the diagnostic analyses performed for performance evaluation of photochemical grid models determines the sensitivity of model predictions to variations in various meteorological parameters. For example the wind speeds may be divided by two to determine photochemical model sensitivity to wind speeds.

Performance evaluation for SAIMM model results was based on graphical comparisons with meteorological data. These results are documented in the 1998 SIP. Comparisons were made between hourly predictions and measurements of wind speed and wind direction at selected monitoring sites. Several attempts were made to replicate the observed wind fields, each time increasing the strength of the nudging coefficients used for FDDA until the wind fields were deemed to be adequate. However, the strong nudging with FDDA produced "many anomalous divergent zones that could not be explained from a physical perspective" (Environ, 2001).

For the photochemical model performance evaluation of meteorological data, a large number of UAM-V model sensitivity analyses were made with various modifications to wind speeds, vertical diffusivity (Kv) values and nudging coefficients. Also tested was the hourly variation of the Kv values. These sensitivity analyses were developed to attempt to obtain better photochemical model performance for the August 16-20, 1993 episode. None of these analyses indicated that reasonable variation of the meteorological parameters would significantly improve photochemical model performance.

After the completion of the technical work for the SIP that TNRCC submitted to EPA in December 2000, a number of individuals and groups raised concerns about the accuracy of the SAIMM modeling used for development of the SIP. TNRCC contracted ENVIRON to model the September 6-11, 1993 episode used for SIP development with the Regional Atmospheric Modeling System (RAMS) and MM5 (ENVIRON, 2001)

RAMS

RAMS is a state-of-the-science non-hydrostatic prognostic meteorological model. This is a numerical prediction model that simulates atmospheric circulations at scales from the hemisphere to turbulent eddy simulations of the planetary boundary layer (PBL). It has been used for operational weather forecasting, air quality regulatory applications, and basic research. For these applications it has typically been used with horizontal scales that range from 2 km to 2000 km. It has also been used for horizontal spacing of much smaller scales to simulate boundary layer eddies with 10 m to 100 m spacing, building simulations with 1 m grids and wind tunnel simulation with 1 cm grids.

The model generates the following fields for each grid cell and each reporting time interval (usually one hour) of the simulation:

- Horizontal wind components
- Vertical wind component

- Potential temperature
- Specific humidity

MM5

MM5 is the fifth generation NCAR/Penn State Mesoscale Model that was originally developed by Penn State and has been enhanced a number of times. It is a state-of-the-science non-hydrostatic, prognostic model that can perform calculations over a grid with multiple nests with one-way or two-way interaction. It is more completely described in Dudhia, 1993 and Grell et al., 1994. MM5 uses primitive equations and a terrain following approach to simulate mesoscale and regional-scale atmospheric circulations. Several different PBL parameterization schemes are available for use in the model that represent sub-grid-scale vertical turbulent fluxes of heat, moisture and momentum. Each approach has a surface energy budget equation to predict ground temperature based on solar insolation, atmospheric path length (solar angle), water vapor, cloud cover, longwave radiation and surface/soil characteristics. The surface properties of albedo, roughness length, moisture availability, emissivity and thermal inertia are defined from a table look up approach based on 25 different categories of land use. MM5 has rarely been run for horizontal grid spacing less than about 4 km, but it had been successfully tested down to 1.33 km by Nielsen-Gammon and Naumann (2000). ENVIRON successfully ran it using a subgrid horizontal spacing of 1.33 km (ENVIRON, 2001). MM5 generates meteorological fields for each grid cell for each reporting time period similar to those developed by RAMS.

Several iterations of both RAMS and MM5 were run to develop alternate sets of meteorological parameters for the September 8-11, 1993 episode (ENVIRON, 2001). Both were run with grid structures similar to the one used for SAIMM, except 41 vertical layers were used and the lowest layer was 10 m high. Both models were also run with a horizontal spacing of 1.33 km over a sub domain of the 4 km domain. When these meteorological parameters were run in CAMx, the model produced ozone results that were similar to those obtained from running CAMx with SAIMM data. This indicates that simply using another meteorological model would not significantly improve CAMx model performance (ENVIRON, 2001) for the September 8-11, 1993 episode.

In 2000 TNRCC began moving toward using MM5 for meteorological modeling. A new computer system was purchased that had sufficient storage capacity and computation capacity to run MM5 for modeling domains in Texas. TNRCC staff has been trained at NCAR and John Nielsen-Gammon is running the model at TNRCC for the August 23-September 1, 2000 episode, which will be used for photochemical grid modeling.

2000 Episode

The TNRCC has elected to use the fifth generation NCAR/Penn State Mesoscale Model (MM5) for meteorological modeling, and in this model the 2-way nested horizontal grid sizes are nested by a factor of three. TRNCC has selected a Texas standardized grid (TSD) for use in meteorological and photochemical model applications in Texas. A horizontal 4 km grid structure was selected to cover the HG nonattainment area. The second nested grid surrounding the 4 km grid cells has a horizontal spacing of 12 km. The third nested grid, surrounding the 12 km grid cells, has a horizontal grid spacing of 36 km. The fourth nested grid surrounding the 36 km grid has a horizontal spacing of 108 km. This grid is illustrated in Figure 17.

Figure 17. The Texas Standardized Grid as used for modeling the August 23 - September 1, 2000 episode

.

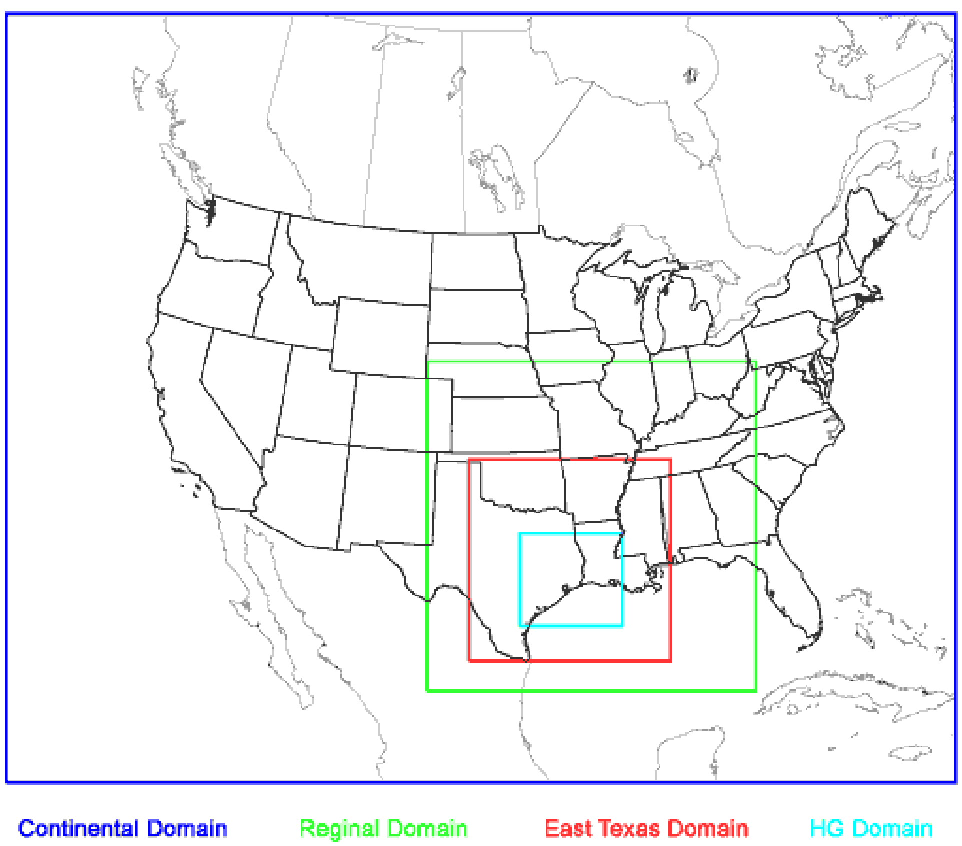

Under TNRCC contract, ENVIRON (ENVIRON, 2001a) has developed an objective, formalized approach for performance evaluation of meteorological modeling. This

guidance. What follows is a very brief summary of this complex process. Readers will find more details in the report referenced above and in Appendix A of this report. The

placed in the meteorological modeling results that will be used in the photochemical grid modeling. The approach focuses on the model results for three-dimensional wind,

Rigorous performance evaluation can be divided into scientific evaluation and operational evaluation.

meteorological processes simulated by it are consistent with prevailing theory, knowledge of physical processes, and observations. The goal is to determine if the

observations, and to provide insight into the proper model options to use for specific applications. The detailed data sets collected during TexAQS are currently being used to

This section of the report will focus on operational evaluation, which evaluates the model application to a specific episode that will be used for photochemical grid modeling. The

performed for the September 13-20, 1999 episode that is being used for photochemical modeling for five areas in Texas that have not been designated nonattainment. There are

Qualitative Analyses

The first step is to perform qualitative assessment of model performance based on

(NWS) and others. Most commonly used are maps of winds, temperature, pressure, and precipitation patterns at the surface and for selected levels aloft. These analyses are to

Environ has used model results at the surface, 850 mb, and 500 mb levels to be consistent with analyses from the NWS. Parameters to plot that are suggested by ENVIRON are

- wind vectors,
- temperature,
- sea level pressure (surface maps),
- geopotential height (aloft maps),
- precipitation (to compare to radar data), and
- Comparison of upper air soundings at specific sites to the model prediction.

Examples are shown in figures 18 through 22 (ENVIRON, 2001). Figure 18 is an example of a surface weather chart showing NWS observations, locations of fronts, radar-derived precipitation, and sea-level pressure patterns. Fronts are shown with solid lines and troughs with dashed lines. Winds are depicted with barbs from a circle. Temperature, dew point and pressure are recorded around the wind barbs. Rainfall is represented by shaded areas. Details for the symbols used on the map may be found at http://weather.unisys.com/surface/details.html#surface. The results from the meteorological model shown in Figures 19 thru 21 may be compared to the measurements shown in Figure 18.

Figure 19 is a map of the surface wind barbs showing wind direction and speed predicted by the meteorological model (MM5 in this example). These wind barbs are similar to those shown in Figure 18, except the temperature, dew point and pressure are not presented. The lines are sea-level pressure isobars (lines of equal sea-level pressure) predicted by the meteorological model. Figure 20 is a map of the surface precipitation accumulation patterns predicted by the meteorological model. Figure 21 is a map of the upper air winds predicted by the meteorological model at the level where the pressure is 500 mb The lines show contours of the geopotential height from meteorological model predictions.

Figure 22 is four plots that compare sounding measurements of temperature, humidity, and wind speed and wind direction to corresponding values predicted by the meteorological model.

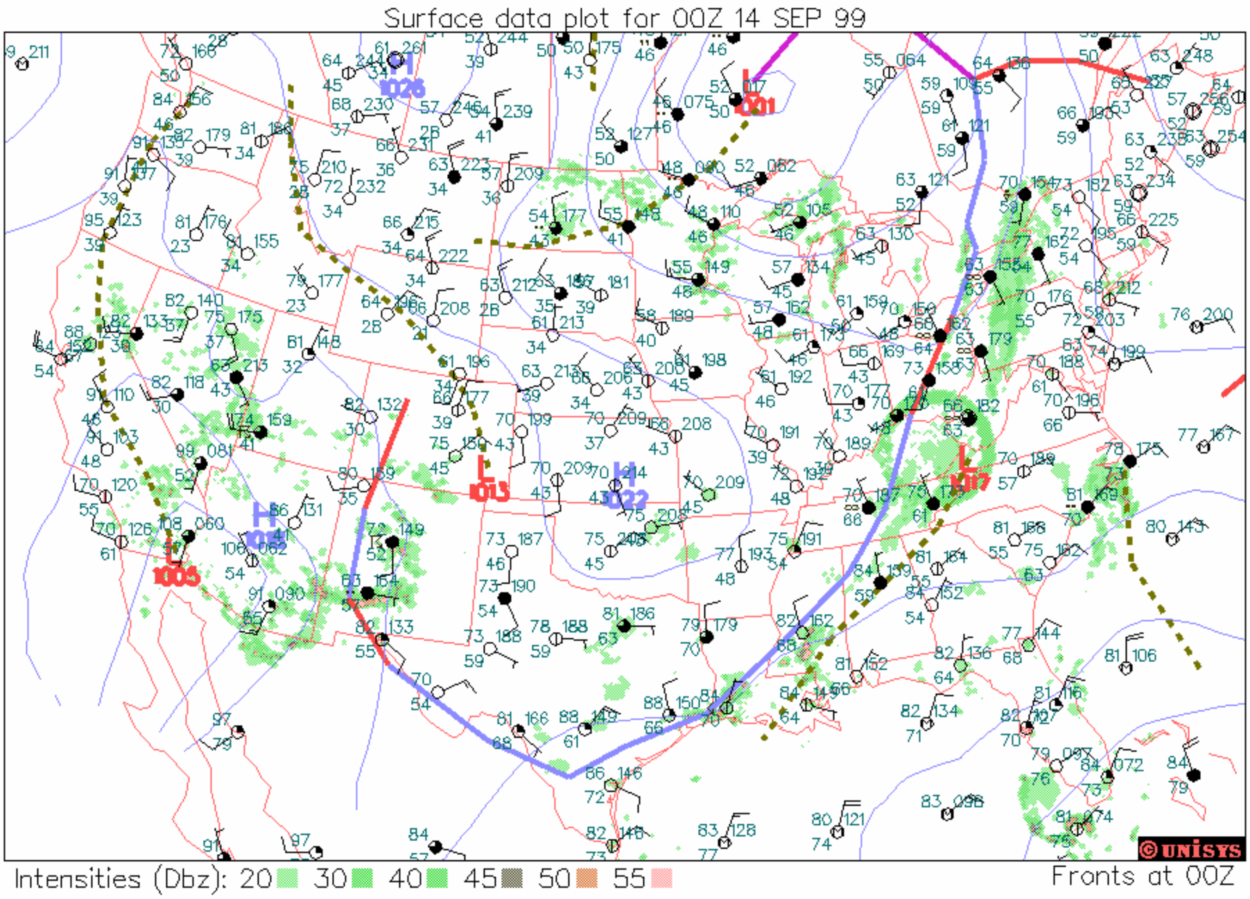

Figure 18. Example of a surface weather chart downloaded from the Unisys Weather http://weather.unisys.com), depicting station observations, fronts, radar-derived precipitation, and sea level pressure patterns. (ENVIRON, 2001)

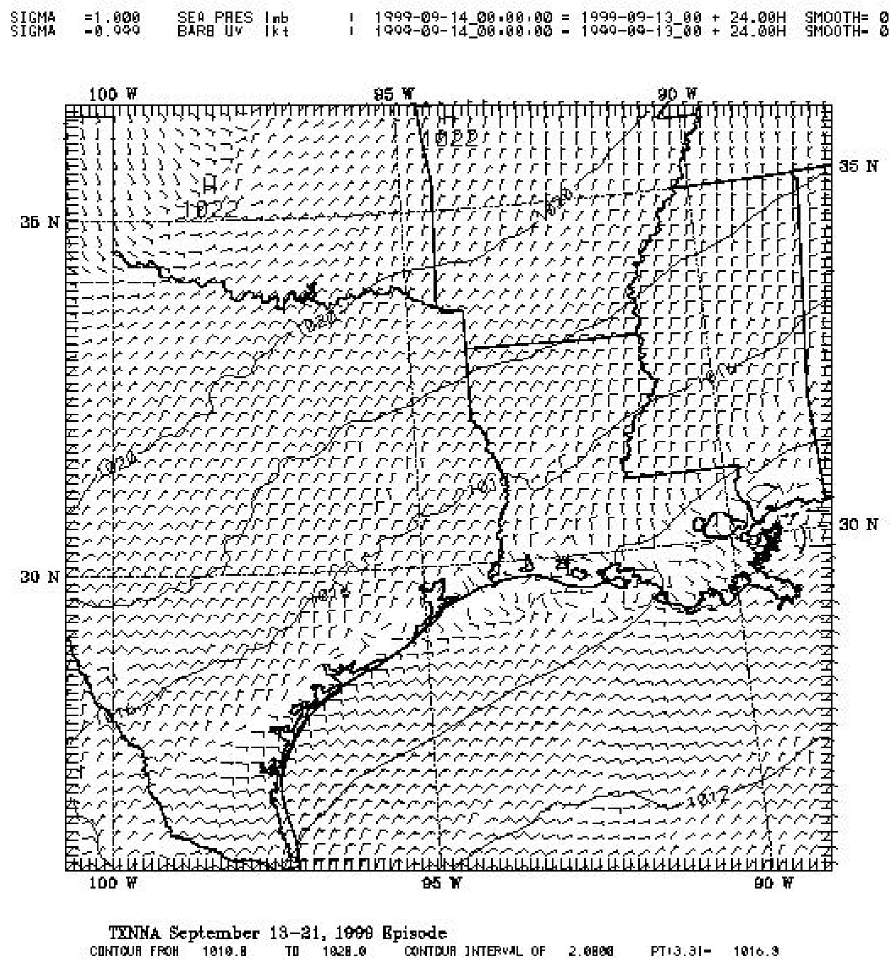

Figure 19. Example plot of MM5 predictions from the GRAPH utility. Shown are surface wind barbs and sea-level pressure isobars

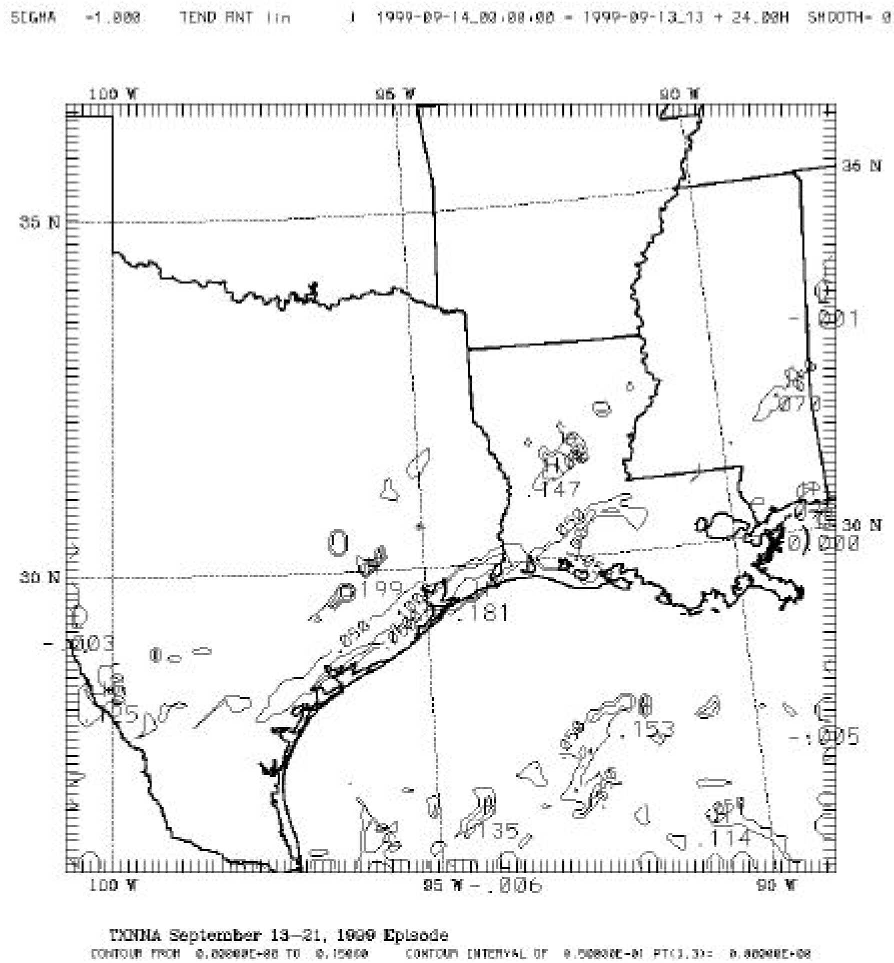

hour surface precipitation accumulation patterns. (ENVIRON,2001)

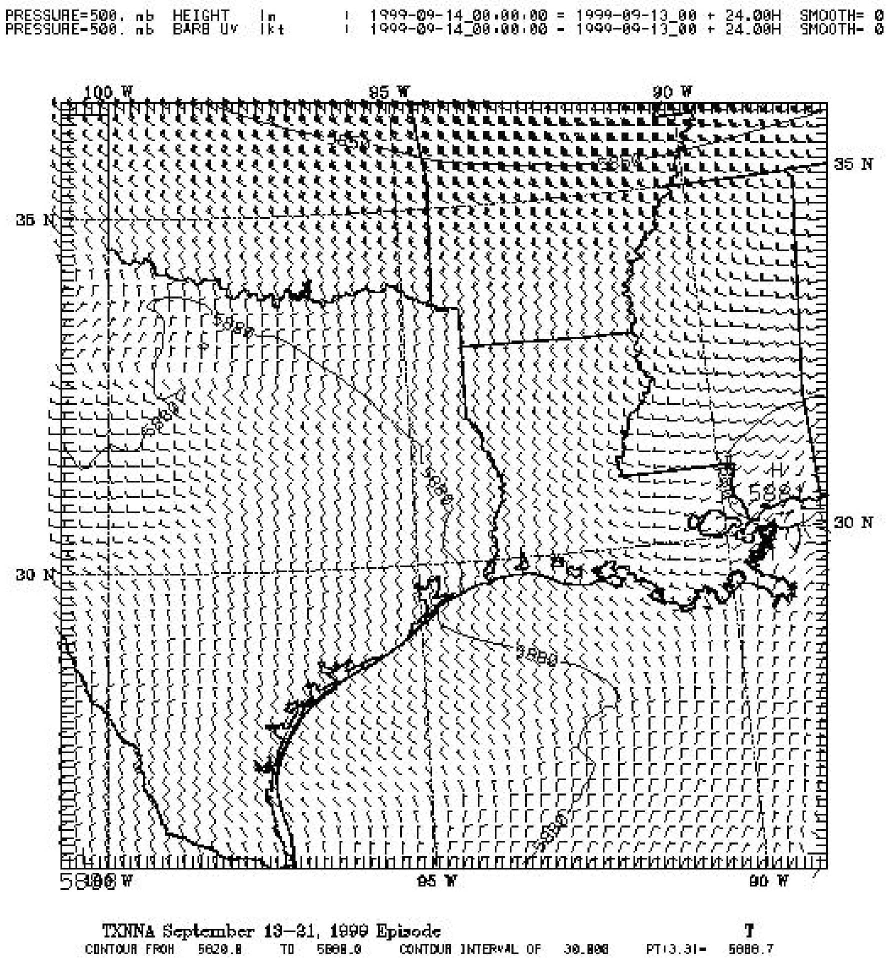

Figure 21. Example plot of MM5 predictions from the GRAPH utility. Shown are 500 mb wind barbs and geopotential height (MSL) contours (ENVIRON, 2001)

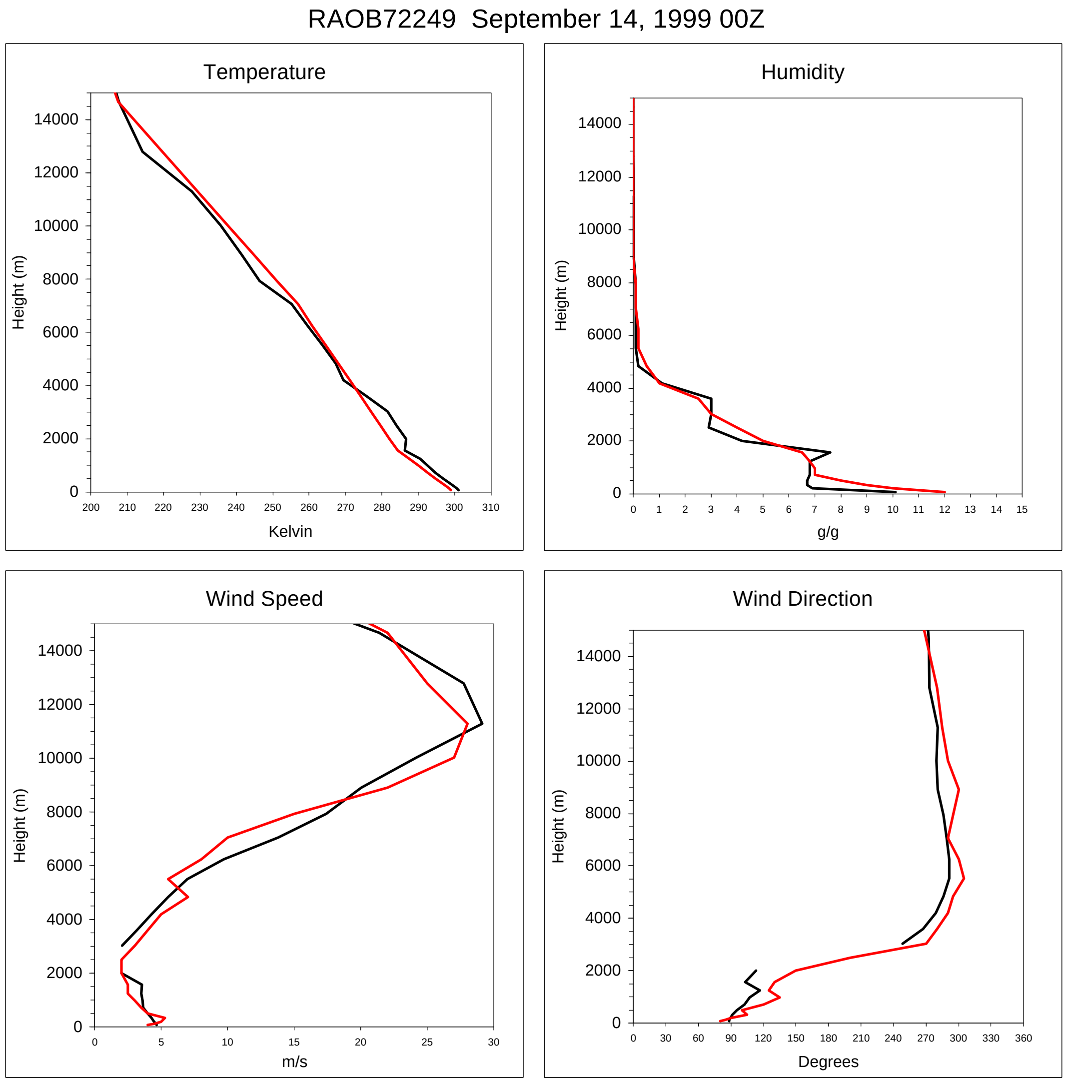

Figure 22. Example of sounding data plotted for the DFW rawinsonde. Measurement data are shown in black, MM5 predictions are shown in red (ENVIRON,2001).

Statistical Analyses

The statistical analyses portion of the operational evaluation is based on results from a computer program developed by ENVIRON named METSTAT (ENVIRON, 2001). This program generates pairings of observations and predictions and calculates statistics between these. It presents tabular and graphical results that are presented as time series and bar charts. The underlying purpose of the METSTAT package is to evaluate and optimize the performance of meteorological models. ENVIRON has proposed a preliminary set of performance goals.

The statistical measures are calculated for:

- Wind speed
- Wind direction
- temperature
- surface humidity
- boundary layer humidity

.

The statistics are reported in absolute terms rather than in percentage terms.

The statistical measures are summarized below. Precise formulations may be found in Appendix A and the ENVIRON report.

- Mean observation – calculated for all monitoring sites
- Mean Prediction – calculated for each site used for mean observations
- Regressed prediction – a least square regression is developed for the predicted values. Then the regressed prediction is the value from the regression curve that fits each corresponding observed value
- Bias error – mean difference between pairings of predicted and observed data over a region – hourly or daily periods
- Gross error –mean absolute value of difference between pairings of predicted and observed data over a region – hourly or daily periods
- Root Mean Square Error (RMSE) – the square root of the mean of the squared difference between pairings of predicted and observed data over a region – hourly or daily periods
- Systematic Root Mean Square Error (RMSES) – the square root of the mean of the squared difference between pairings of the regressed prediction and observed data over a region – hourly or daily periods
- Unsystematic Root Mean Square Error (RMSEU) – the square root of the mean of the squared difference between pairings of the regressed prediction and the prediction at each measurement site over a region – hourly or daily periods.
- Index of agreement (IOA) – at each monitoring site, calculate the sum of the absolute value of the difference between the prediction and the mean of the observations and the absolute value of the difference between the observation and the mean of the observations. These sums are added over all monitoring sites and divided into the square of the RMSE. Then this value is subtracted from 1.

METSTAT calculates the following statistics for each hour and each day desired:

Wind speed, temperature, and humidity

- Mean observation
- Mean prediction
- Bias
- Gross error
- RMSE
- RMES
- RMSEU
- IOA

Wind direction

- Mean observation
- Mean prediction
- Bias
- Gross error

The proposed performance goals are shown in Table 1. These performance goals were based on a comparison of statistical summaries of the results of nearly thirty regional meteorological model simulations used to drive photochemical models in almost every area of the country. The performance goals were chosen to establish a level of performance that most past modeling has achieved to filter out those applications that exhibit particularly poor performance. It should be stressed that these goals are guided by the results of meteorological models that have been accepted and used in support of historical regulatory photochemical air quality modeling efforts. The performance goals will require refinement as the state of the science of meteorological modeling improves. Furthermore, the statistics were only calculated for results on the 12-km grids. For photochemical modeling performance goals at grid resolutions of 4-km of less may require higher accuracy and will likely be significantly different than those at 12-km.

Table 1. Proposed Daily Performance Goals

Wind speed	RMSE	≤ 2 m/s
	Bias	≤ ± 0.5 m/s
	IOA	≥ 0.6
Wind direction	Gross error	≤ 30 degrees
	Bias	≤ ± 10 degrees
Temperature	Gross error	≤ 2 degrees K
	Bias	≤ ± 0.5 degrees K
	IOA	≥ 0.8
Humidity	Gross error	≤ 2 g/kg
	Bias	≤ 1 g/Kg
	IOA	≥ 0.6

The ENVIRON report provides the results of the performance evaluation for the application of MM5 to an episode for September 13-20, 1999. The modeling domain is shown in Figure 4. The results for the 12 km grid and two 4 km subgrids over the Dallas/FtWorth and HG areas are reported. Figure 23 is the time series for hourly statistical comparisons between observed and predicted wind speeds and direction over the 4 km HG subgrid.   Figure 24 is the corresponding data for temperatures over the 4 km HG subgrid. For the same data set bar graphs illustrating daily statistics are shown in Figure 25 and Figure 26.

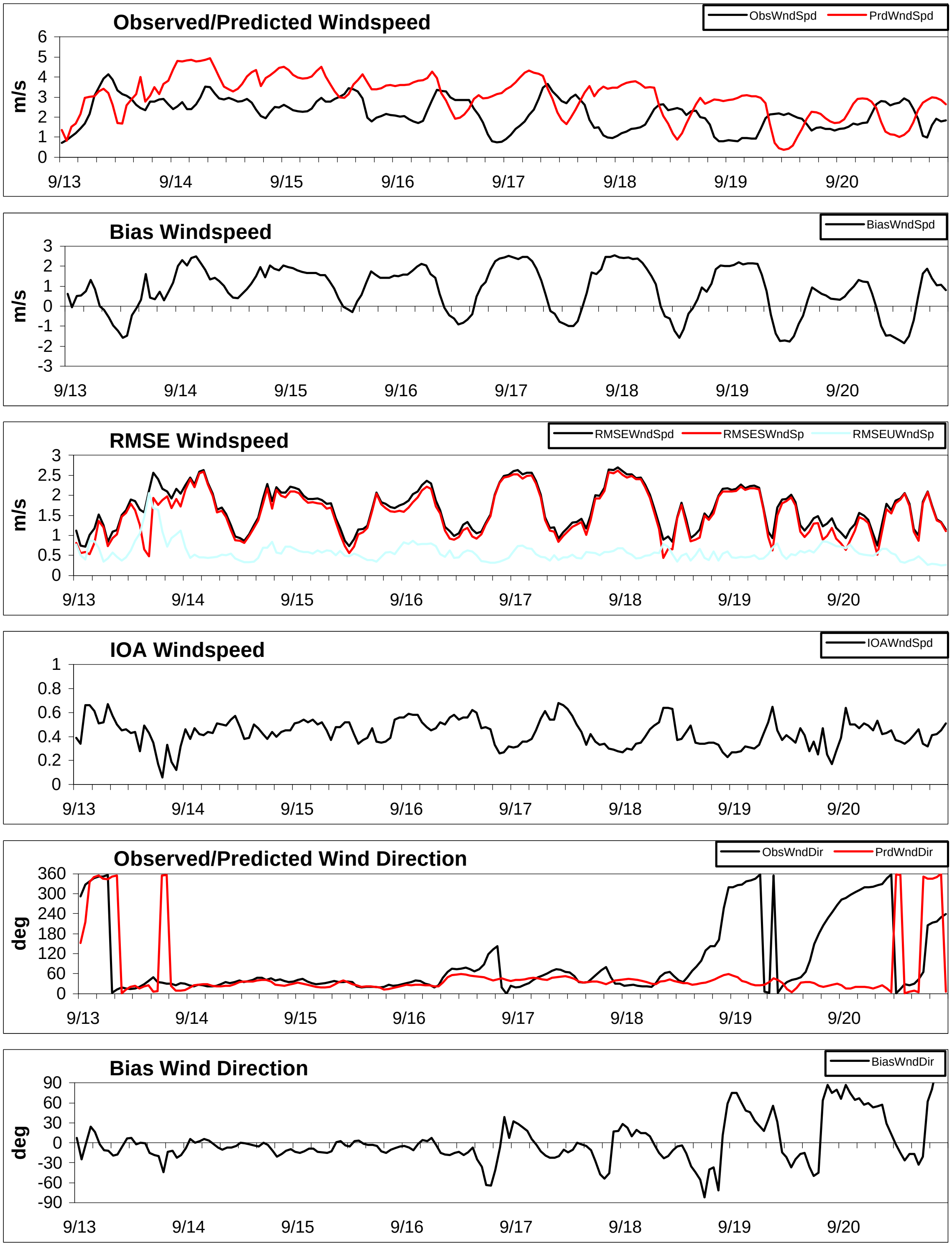

Figure 23. Hourly region-average observed and predicted (Run 1) surface-layer winds and performance statistics in the HG/BPA subregion of the 4-km MM5 domain over the September 1999 modeling episode. RMSE is shown for total, systematic (RMSES) and unsystematic (RMSEU) components.(ENVIRON, 2001)

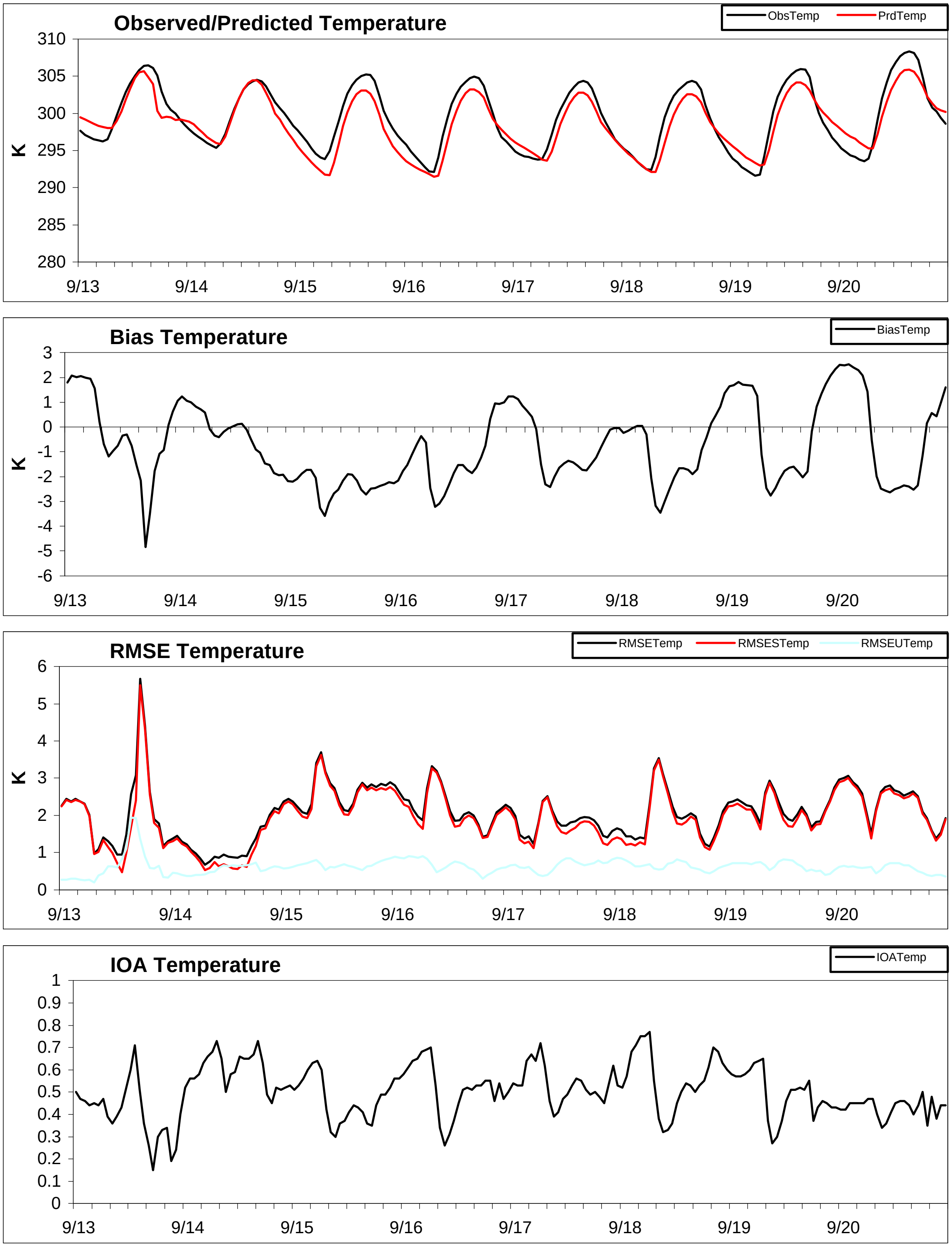

Figure 24. Hourly region-average observed and predicted (Run 1) surface-layer temperature and performance statistics in the HG/BPA subregion of the 4-km MM5 domain over the September 1999 modeling episode. RMSE is shown for total, systematic (RMSES) and unsystematic (RMSEU) components. (ENVIRON, 2001)

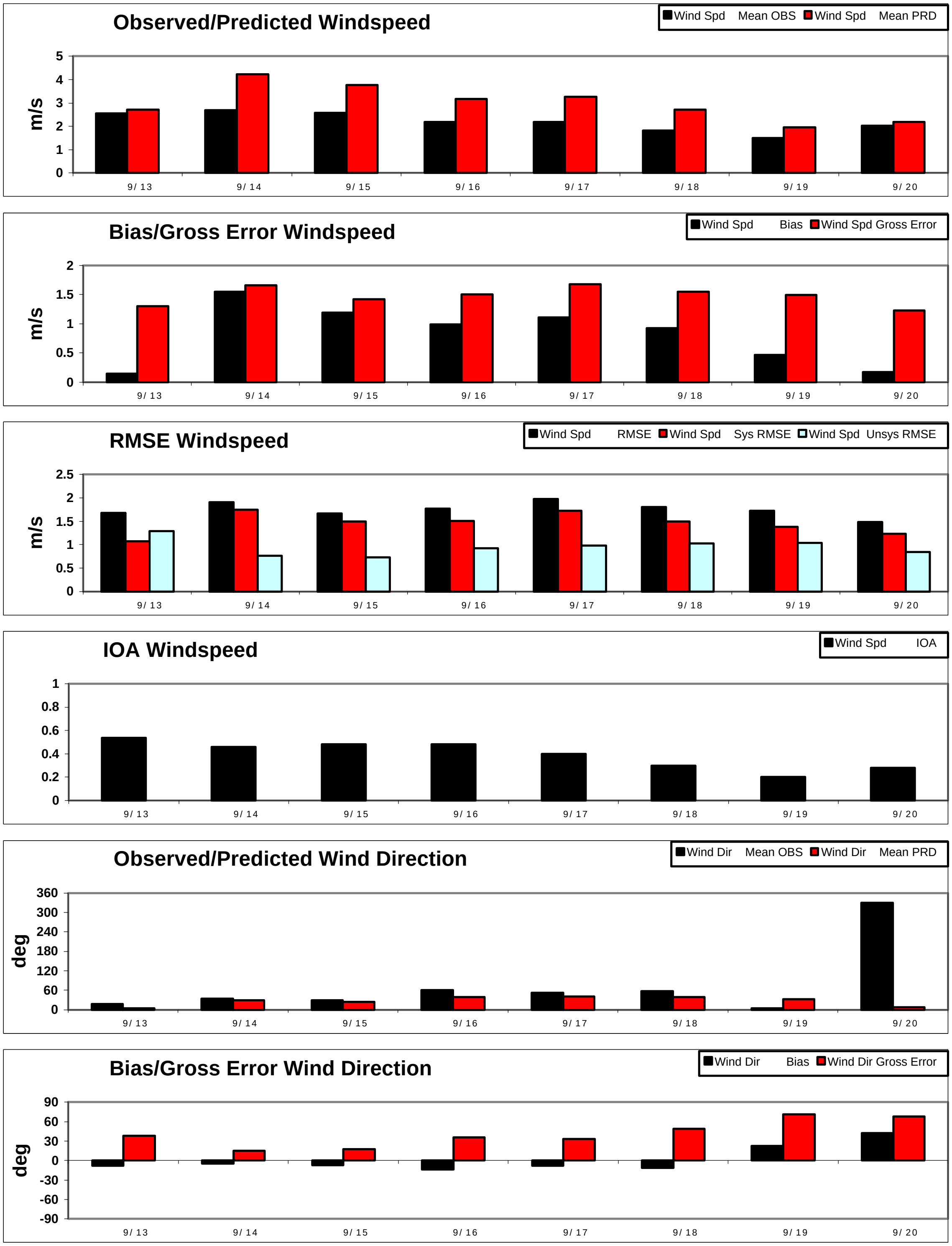

Figure 25. Daily region-average observed and predicted (Run 1) surface-layer winds and performance statistics in the HG/BPA subregion of the 4-km MM5 domain over the September 1999 modeling episode. RMSE is shown for total, systematic and unsystematic components (ENVIRON,2001).

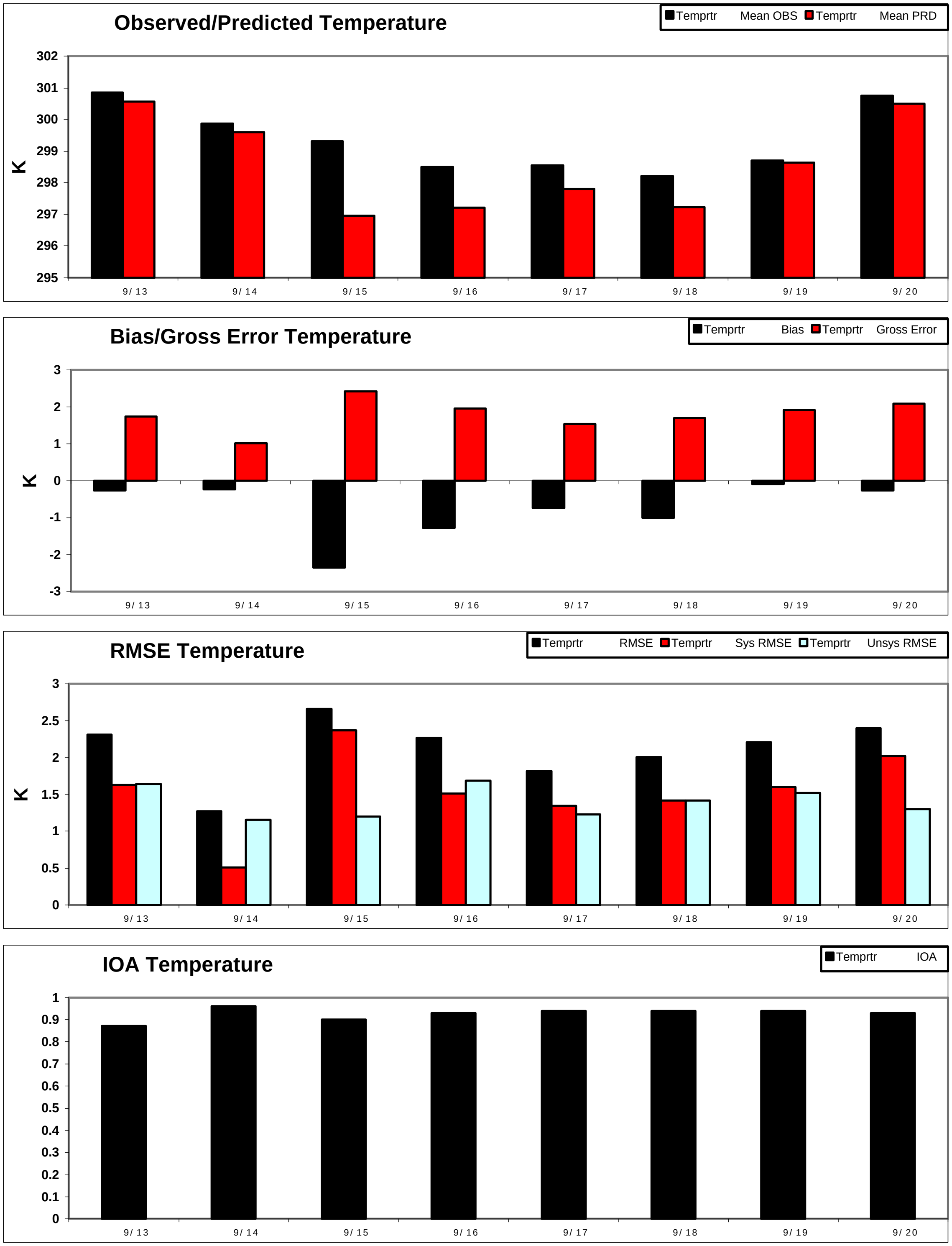

Figure 26. Daily region-average observed and predicted (Run 1) surface-layer temperature and performance statistics in the HG/BPA subregion of the 4-km MM5 domain over the September 1999 modeling episode. RMSE is shown for total, systematic and unsystematic components (ENVIRON, 2001).

This set of criteria can also be used to evaluate the performance of any model to simulate any episode. For example it could be used to evaluate the relative performance of the SAIMM, RAMS, and MM5 modeling of the September 8-11, 1993 episodes (Environ, 2001a). The ENVIRON METSTAT process is also being used to evaluate the performance of the MM5 modeling for the August 23 - September 1, 2000 episode. These performance evaluation procedures could be used to evaluate various model sensitivity runs of the same episode using variations in model inputs. This would allow the selection of the best set of model parameters, grid structure and amount and frequency of nudging to be used for preparation of the meteorological parameters for photochemical grid modeling. Once the performance of the meteorological model is deemed to be adequate, then the meteorological model is used to develop inputs for photochemical grid modeling. Additional performance evaluation of the meteorological inputs is conducted during the performance evaluation of the photochemical grid model.

In addition to qualitative and statistical comparisons between predictions and observations, comparisons between results from model runs with different parameterizations or results from different models should be performed. For example Figure 27 (Environ, 2001b) shows the surface wind file determined by RAMS at 1800 UTC on September 8, 1993. Figure 28 shows the surface wind fields predicted by MM5 at the same time. RAMS develops strong onshore winds, a convergence zone just inland from the coastline and strong northerly winds in inland areas. In contrast, MM5 generates strong wind parallel to the coastline, no convergence zone, and nearly calm winds over land areas. It is clear that there are major differences in wind speed and directions in these simulations, especially along the coast.

Another example of significant differences is shown in Figures 29 and 30. Both these figures show the results for 1200 UTC on September 9, 1993. It is clear that MM5 is predicting thunderstorms and outflow boundaries in two places that were not predicted with RAMS. Performance evaluation procedures could be used to determine which simulation is the better one to use for photochemical modeling. A key result would be to determine how the photochemical grid model performed with each set of meteorological data.

Figure 27. RAMS T5 surface wind field for September 8, 1993 1800 UTC. Vectors plotted every other grid point. (ENVIRON).

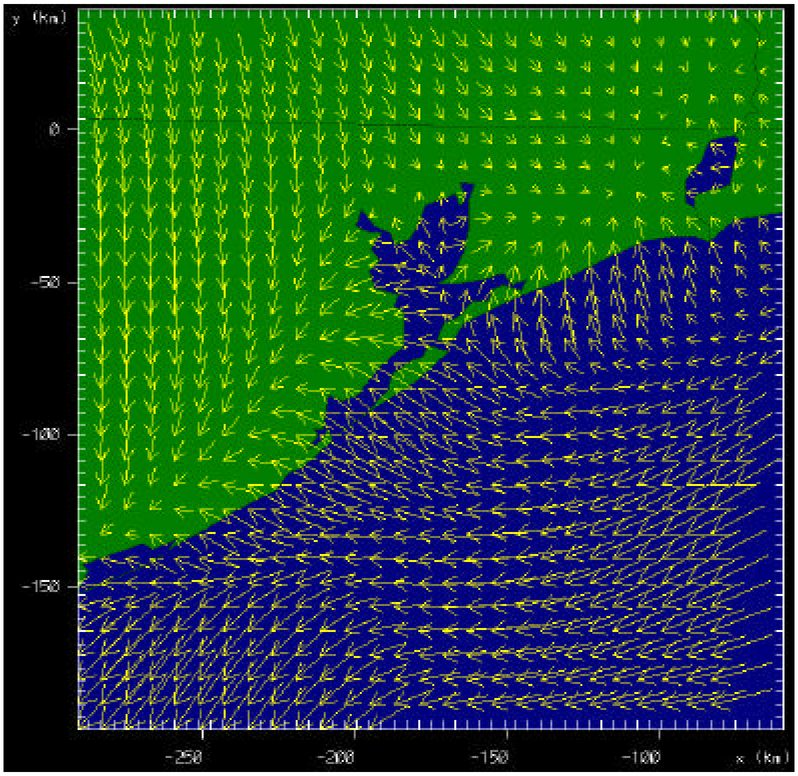

Figure 28. MM5 G3 surface wind field September 8, 1993 1800UTC. Vectors plotted every other grid point. (ENVIRON).

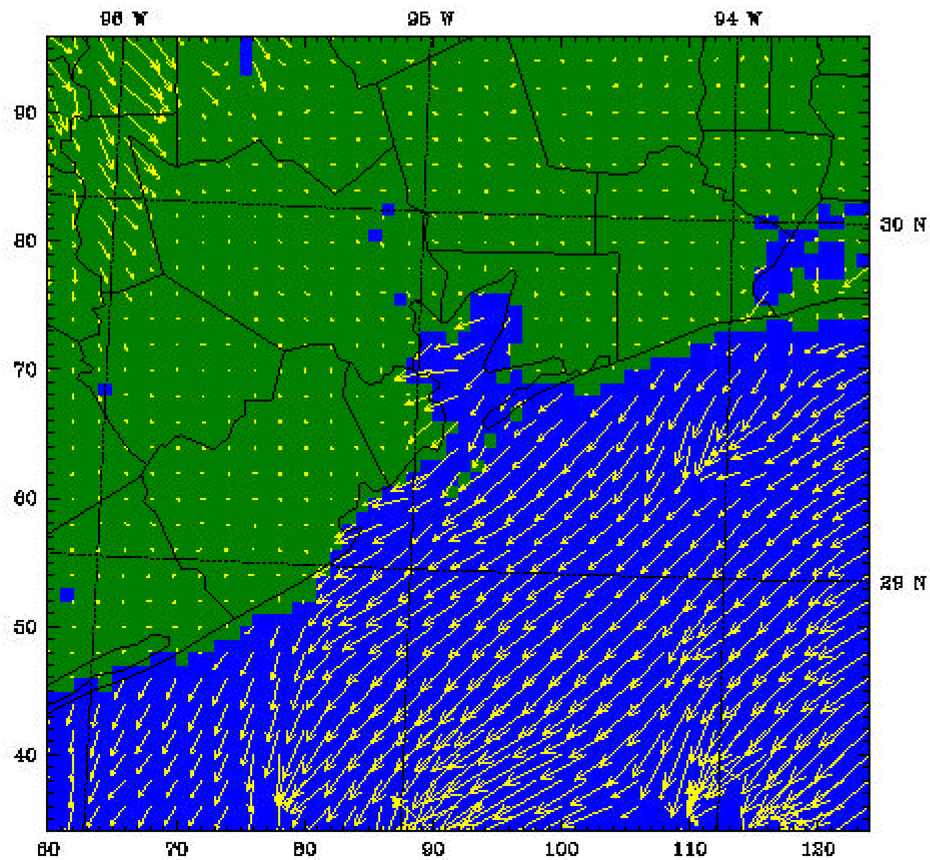

Figure 29 .MM5 G3 surface wind field September 9, 1993 1200 UTC. Vectors plotted every other grid point. (ENVIRON).

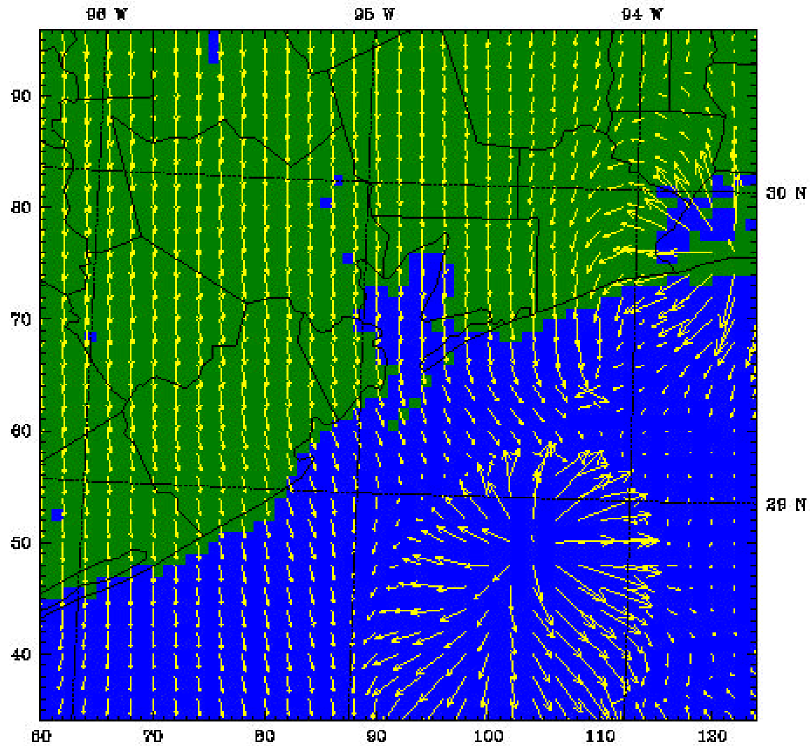

Figure 30. RAMS T5 surface wind field September 9, 1993 1200 UTC. Vectors plotted every other grid point. (ENVIRON).

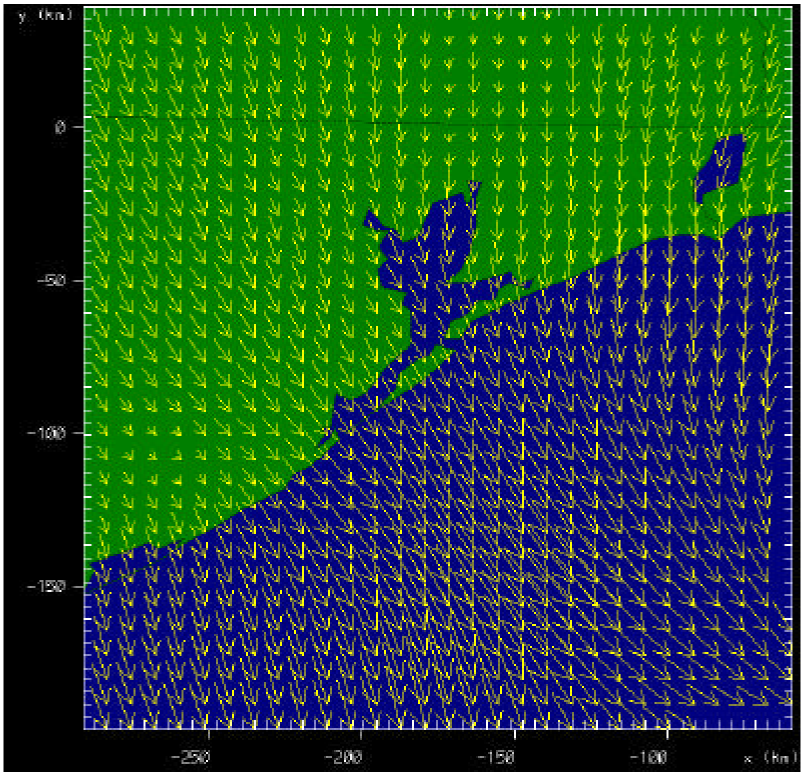

Performance methodology procedures should also be developed to evaluate the ability of the model to predict the location, timing and movement of clouds. Cloud cover strongly affects surface temperature and solar insolation by modifying the energy and radiation balances. Accurate temperature and solar radiation data are very important for the estimation of biogenic emissions, which are strongly influenced by these parameters. In addition, the reaction rates for many gas-phase chemical mechanisms used in the photochemical model depend on the solar intensity and temperature. Given the uncertainties inherent in using a grid-based model to predict the time and location of clouds, it is not clear how a statistical comparison between model output and observations could be performed at this time; therefore, a qualitative comparison would be appropriate until the necessary quantitative approach is developed.

Incoming solar radiation (insolation) can have significant variation across a modeling domain when clouds are present. This variation can dominate other terms in the surface energy budget. In order to provide a robust measure of model performance it would be useful to compare model estimates of solar radiation with both in situ pyranometer measurements and also satellite estimates of insolation. Satellite measurements of insolation are relatively robust since the reflected radiation measured by the satellite provides a good measure of the solar radiation not reaching the ground. This is especially true for higher sun angles when the insolation is most important.

In addition to evaluating the statistical performance of the model using point-by-point comparisons (RMSE, MAE, ME and Index of Agreement for wind speed, and RMSE, MAE and ME for direction), it would be useful to consider an evaluation that is more directly linked to how wind errors lead to transport errors for atmospheric pollutants. This can be accomplished by comparing model predictions to observations averaged through the full boundary layer.

Key Scientific Questions

The historical summary of meteorological modeling and photochemical air quality modeling for the HG area reveals that the meteorological models have been continually improved since their initial application more than a decade ago. However, a number of uncertainties related to the ability of the meteorological models to accurately replicate observations remain. The most significant issues that need to be addressed in the Accelerated Science Evaluation are:

1. What meteorological conditions are associated with high ozone concentrations in the Houston Galveston area during the Texas Air Quality Study?

2. What atmospheric processes lead to the conditions conducive to ozone formation?

3. Can available meteorological models adequately simulate these processes?

4. How can observations best be assimilated into a meteorological model to enhance its representation of these processes?

5. What is the minimum set of routine observations needed to adequately simulate the meteorological parameters used for photochemical grid modeling?

6. Are linkages between meteorological and photochemical grid models accurately transferring wind field information?

The robust data set collected during TexAQS can be utilized to address all of these questions. These data are being used to evaluate and improve the performance of meteorological models and to determine the best approaches to develop accurate data inputs for photochemical modeling.

1. What meteorological conditions are associated with high ozone concentrations in the Houston Galveston area during the Texas Air Quality Study?

The conceptual model developed by TNRCC (refer to "Meteorological Conditions Correlated with High Ozone in the HG area" discussed previously in this report) was primarily based on analyses of surface measurements collected at approximately 25 routine monitoring stations located in the HG area. The additional measurements collected from the greatly enhanced monitoring network employed during TexAQS are already providing new insights into the meteorological conditions that lead to the formation of ozone in the HG area. In particular, the observations that provide information on the vertical structure of atmospheric winds (e.g., radar wind profilers) have been especially useful.

The following discussions summarize the meteorological conditions during the period from August 25 - September 1, 2000. This period has been identified as the primary episode during TexAQS that will be used for photochemical modeling, and has been studied in detail by J. Nielsen-Gammon (Nielsen-Gammon, 2001, 2002a, 2002b). While the preliminary results of this study add significantly to the understanding of atmospheric processes in Southeast Texas, it is premature to incorporate specific information into the conceptual model of meteorological conditions that lead to the formation of ozone in the HG area. Additional analyses relating the location, spatial extent, and timing of high ozone concentrations to the prevailing meteorological conditions are required and will be performed. These analyses will undoubtedly lead to an improved understanding of these conditions. The results to-date are summarized here as a work-in-progress and the reader is encouraged to read the Nielsen-Gammon report for additional details.

Most of the days during the August 25 - September 1, 2000 episode were characterized by maximum temperatures well above normal, decreased absolute humidity, and a lack of widespread convective activity. The winds followed a regular diurnal (24 hour daily) cycle. The cycle was observed offshore, aloft, and along the coastline, and was characterized by the strongest onshore winds during the afternoon and early evening and strongest offshore winds during the morning. This behavior is attributed to the interaction of the sea breeze and the Earth's rotation at a latitude where the so-called inertial period is slightly greater than one day.

Further analysis of the three-dimensional wind structure on these days revealed that the episode was composed of two distinct meteorological regimes. The behavior of the winds was extremely sensitive to whether the large-scale winds were onshore or offshore. Regime I occurred from August 25 to 29 when the large-scale winds near the surface were onshore. Composite winds during Regime I demonstrate a diurnal circular pattern at all levels, as shown in Figure 31. (Note: Although the diurnal rotation of the winds on the days during each Regime were similar, the surface wind trajectories varied day-to-day depending on the strength and direction of the large-scale winds, i.e., each day was characterized by unique wind speeds and wind directions.) There is a time lag of one to two hours in wind directions between the surface and higher layers and the wind speed is relatively constant with height. Thus, there is very little vertical wind shear. The amplitude (size) of the circle is assumed to be determined by the amount of daytime heating and nighttime cooling.

Figure 31. Time hodograph showing composite diurnal wind cycle, Houston Southwest Airport profiler. Winds are averaged for each hour on August 25, 27, 28 and 29, 2000. The U (east-west) component of the wind is on the horizontal axis. The V (north-south) component of wind is on the vertical axis; each grid box represents 1 m/s. The altitude of each layer of the hodograph is indicated by the legend. The wind at a given level and hour can be represented as a vector that begins at the origin and ends at the appropriate point on the curve. For example, the red vector shown in the figure corresponds to a wind blowing from the southeast at 6.4 m/s. Due to the number of levels displayed in the figure, the hours represented by each point on the hodographs have not been labeled. Winds during this period are generally southerly, and the strongest southerly winds occur between 9 pm and midnight CST. The trace of the mean winds rotates clockwise on the hodograph so that early morning winds are from the southwest and late morning winds are light. Data provided by NOAA/ETL. (Nielsen-Gammon, 2001).

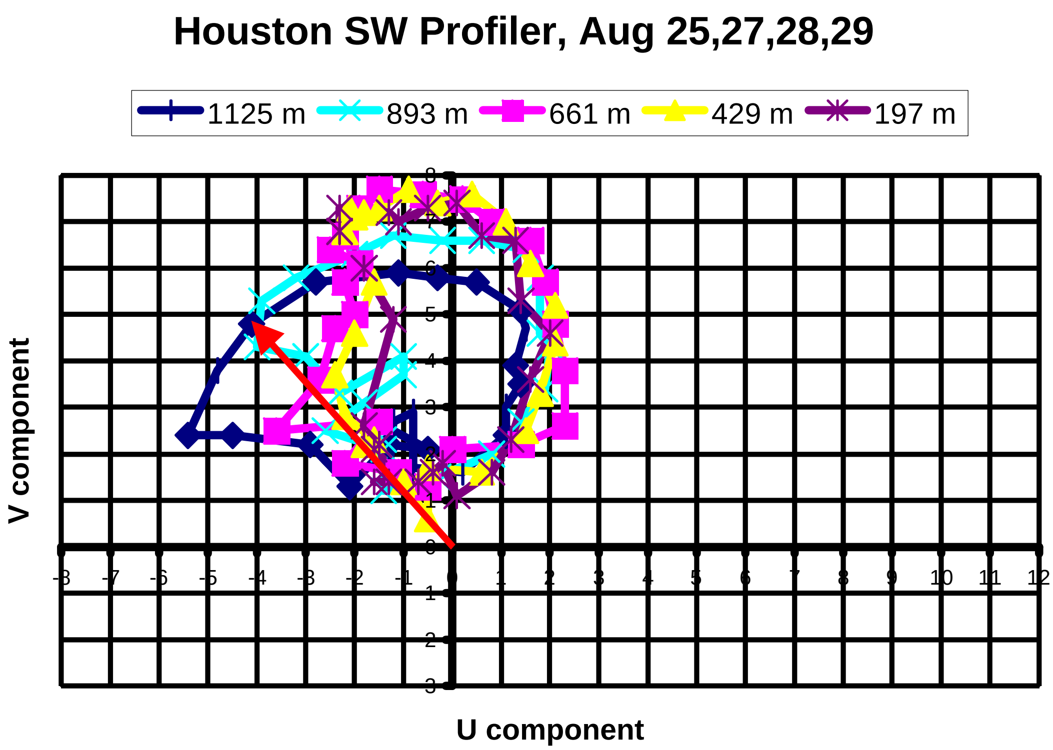

Regime II occurred from August 30 to September 1 when the large-scale winds were parallel to shore or offshore. The composite winds in Regime II are shown in Figure 32. Instead of the regular circle of Regime I, the figure shows an elongated ellipse. This indicates that winds do not vary similarly with height but the diurnal cycle decays to near zero at a height of approximately 1 km above the surface. In Regime I, the difference in the horizontal wind speed between sunrise and sunset was only a few m/s, while for Regime II the horizontal wind speed changes by more than 10 m/s. Furthermore, the winds during Regime II are mostly westerly instead of southerly.

Since the large-scale winds blew parallel to the coast during Regime II, there was little mixing of the air over land with that over water and the temperatures over land warmed considerably. The resulting difference between surface air temperatures over land and sea generated a strong land-sea temperature gradient. This temperature gradient caused a pressure drop at low levels over land, leading to a situation known as adverse shear. Normally, wind speeds increase with altitude in the boundary layer. Adverse shear is characterized by strong winds at low levels, with decreasing (or reversing) direction aloft, and is a classic indicator of the nocturnal low-level jet.

During the day, the high winds near the surface are mixed with the lighter winds aloft within the well-mixed PBL, leading to relatively lighter average wind speeds. At night, radiational cooling forms a near-surface temperature inversion and the winds aloft decouple from the surface. No longer feeling the effects of friction, the winds immediately above the near-surface layer increase in response to the land-sea pressure gradient, forming the nocturnal low-level jet. In the near-surface layer beneath the shallow inversion, the air is trapped and the winds are very light. During the morning hours after sunrise, the near-surface winds increase dramatically as mechanical mixing due to heating of the earth's surface mixes the stronger winds to the ground for a few hours. As the PBL continues to deepen, the lighter winds aloft decrease the average wind speed in the surface layer. It is hypothesized that the magnitude of the low-level jet is locally enhanced by the diurnal heating cycle. The frictionally induced (inertial) wind cycle is almost exactly in phase with the sea breeze cycle, so the two effects amplify each other.

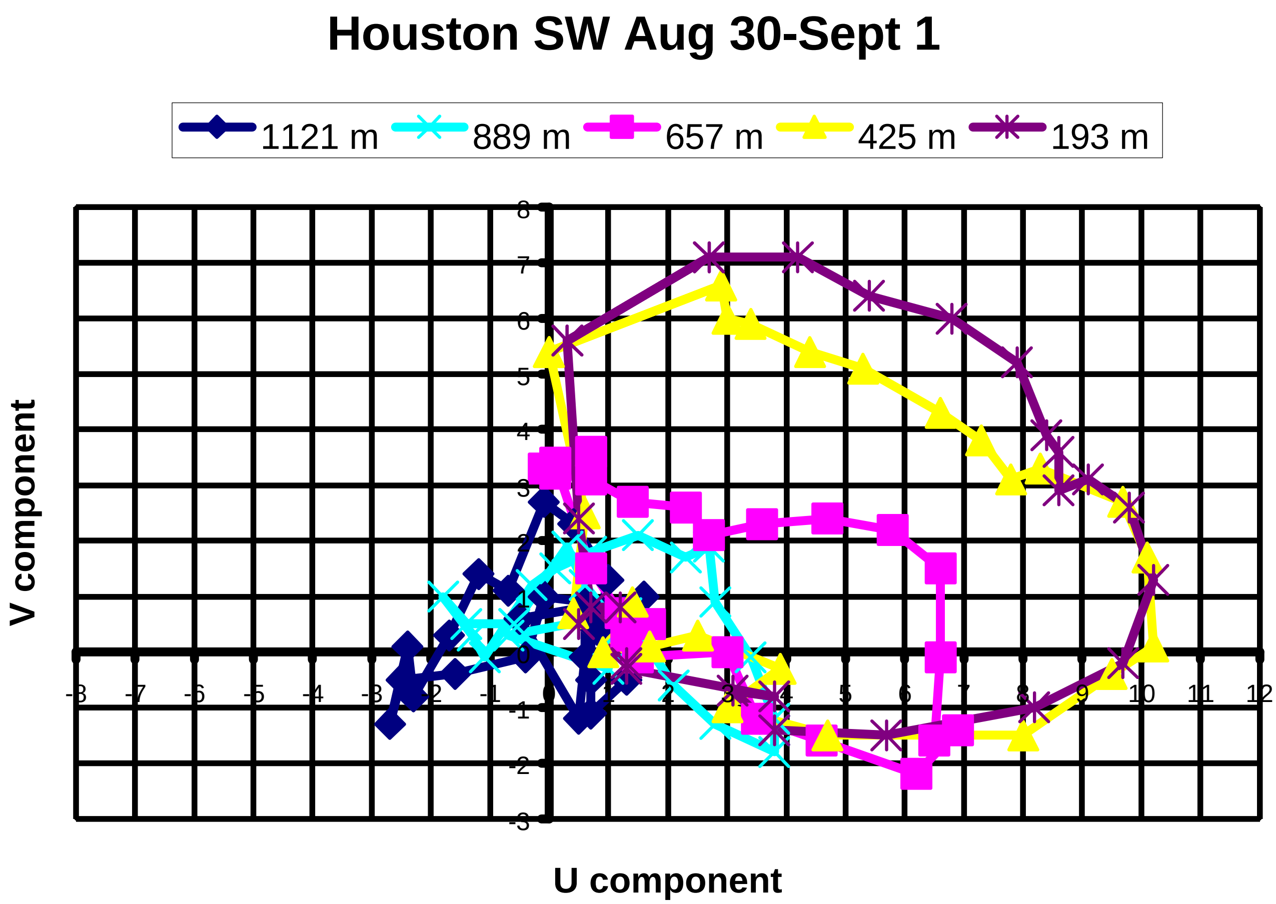

Figure 32. Time hodograph showing composite diurnal wind cycle, Houston Southwest Airport profiler. Winds are averaged for each hour on August 30, 31, and September 1, 2000. The strongest winds are from the west and occur around sunrise at low levels in the atmosphere. During the morning the low-level winds rapidly weaken, and the weakest winds are found in early to mid afternoon. The strong diurnal wind cycle decreases in amplitude to nearly zero at a height of 1 km. Data provided by NOAA/ETL. (Nielsen-Gammon, 2001).

The summary above indicates that the conceptual model should be revised to incorporate results from analyses based on the variability in the diurnal wind cycle. For example, the transport of ozone and ozone precursor compounds will differ significantly between the two Regimes. During Regime I, the winds generally varied little with height, suggesting that air parcels within the lowest km are transported over similar regions. However, the more complex spatial and temporal variation of horizontal wind with height observed during Regime II suggests that air parcels transported into and out of Southeast Texas would follow very different trajectories depending on the starting height above ground. For example, at night, the strong winds just above the surface would transport ozone far from the region while the light winds at the surface would result in little movement. Further analyses should be performed to determine the differences in the meteorological parameters during each Regime between the days when high ozone was measured at surface sites and when it was not measured (e.g. Aug 25, Aug 29, and Aug 30, 2000 compared to Aug 26, Aug 27 and Aug 28, 2000). Measurements from airborne sampling should be incorporated as well. The insight provided by these additional analyses should then be further tested and, if proved accurate, incorporated into the conceptual model.

2. What atmospheric processes lead to the conditions conducive to ozone formation?

The key meteorological conditions contributing to high levels of ozone in southeast Texas include warm weather, little or no precipitation, light large-scale winds, and particular combinations of diurnally-rotating and locally-forced winds that lead to air stagnation, flow reversal, and/or the buildup of ozone in shallow layers over the Gulf of Mexico.

Light large-scale winds in southeast Texas lead to conditions conducive to ozone formation. First, as in other locations, light winds minimize dispersion of pollutants. Second, in southeast Texas, if winds are lighter than the amplitude of the diurnal wind cycle, the wind direction can progress through a complete circle and recirculation or flow reversal takes place. Third, the onshore component of the large-scale wind determines the location and intensity of the sea or bay breeze front. Strong offshore (directed toward water) or onshore (directed toward land) winds prevent sea breeze fronts from forming. Weak offshore winds produce strong sea breeze fronts, which remain near the coastline. Weak onshore winds produce indistinct sea breeze fronts that advance far inland.

Under sunny, warm conditions, light large-scale winds are related to the location and intensity of surface high and low pressure centers. If high pressure is centered over southeast Texas, or if the surface pressure gradient is particularly weak, light winds will be present. If the pressure gradient is large, such as with an intense Bermuda high to the east or a developing dryline trough to the west, winds will remain strong.

The diurnal wind cycle in southeast Texas affects an unusually large area and occurs much later in the day than sea breezes at typical midlatitude locations. According to theoretical studies of the sea breeze (e.g., Rotunno 1983), the uniqueness of the southeast Texas sea breeze is associated with the interaction of the sea breeze and the Earth's rotation at this latitude. The specific pattern and timing of winds is also sensitive to surface friction within the planetary boundary layer. Day-to-day variations in the diurnal wind cycle depend on the magnitude of the heating and cooling cycle over land.

Smaller-scale wind and temperature variations can be critical for development of local-scale convergence zones and buildup of pollutants, such as sometimes have been observed during the morning hours near the ship channel. These variations can be produced by coastline irregularities, land use patterns, irrigation patterns, recent rainfall patterns, and interactions with developing clouds and convection. Some have speculated that the generation and emission of heat from industrial activity may be a significant contributor to convergence in the ship channel area.

3. Can available meteorological models adequately simulate these processes?

During TexAQS, a wide range of regular and special meteorological measurements were collected from multiple observation platforms (e.g., fully instrumented ground stations, buoys, radar wind and boundary layer profilers, rawinsondes). These meteorological measurements provide an unprecedented opportunity to observe the three-dimensional structure and evolution of atmospheric features affecting southeast Texas. These meteorological observations can be used in two ways. First, they can be used to evaluate the performance of meteorological models and to adjust the parameterizations used by models such as MM5. This process is iterative, in the sense that the input parameters to the model may be altered to improve the agreement between observations and modeled fields. Ideally, this process results in refinement of the model so that it accurately simulates all the important processes occurring in nature and can accurately predict the meteorological parameters to be used in the photochemical grid modeling. Second, the observations may be assimilated directly into the model to improve the accuracy of modeled fields through data nudging. As discussed in key scientific question #4, the best approach is to adjust model parameterizations so that the model will correctly simulate all atmospheric processes. Data nudging should only be used as a last resort.

Many of the discussions in this section are focused on the MM5 modeling performed by Nielsen-Gammon for the August 25 – September 1, 2000 episode, which TNRCC intends to use for photochemical modeling if acceptable photochemical model performance is achieved. The significant goals and results-to-date are presented to provide the reader with examples of specific research activities and analyses recently performed to analyze and improve meteorological model performance; however, the final photochemical modeling may require further work with additional meteorological models (such as RAMS) using historical episodes.

The parameters used in MM5 to describe the August 25 - September 1, 2000 episode have been examined, focusing on their ability to predict the diurnal temperature cycle, the interaction of the sea/bay breezes with the large scale wind, the development and evolution of the PBL, and the vertical structure and strength of the nocturnal low-level jet that developed on some days (Nielsen-Gammon, 2001, 2002a, 2002b). *Nielsen-Gammon has found that the critical aspects for proper model configuration include land surface characteristics (e.g., soil moisture, land use type), model vertical grid structure, and the* *algorithm used for parameterization of the PBL. As discussed in key scientific question #4, observational nudging of the three-dimensional large-scale wind field was required to obtain an acceptable MM5 simulation of the winds.* Details on the suggested optimal model configuration and results of the sensitivity modeling may be found in Nielsen-Gammon (2001, 2002a, 2002b).

Surface Temperature

It is well known in the modeling community that MM5 has a tendency to under predict the amplitude of the diurnal temperature cycle (Environ, 2001). The preliminary modeling performed by Nielsen-Gammon for the August 25 - September 1, 2000 episode was used to quantify this tendency for the HG area. The daily maximum and minimum 2-meter temperatures (hourly average) predicted by the model were compared to the minimum and maximum temperatures measured at eight NWS stations for each day of the model simulation. These data are shown in Figure 33 for two slightly different model configurations. MM5 Test Run #2 is identical to MM5 Test Run #1, except that an additional lower vertical surface layer was added to MM5 Test Run #2. The maximum temperatures predicted by both models were virtually identical; however, the minimum temperatures are slightly lower in the MM5 Test Run #2.

The slightly improved performance of MM5 Test Run #2 demonstrates that the additional vertical resolution in the boundary layer slightly improves the performance of the PBL scheme. However, as demonstrated by the average temperature biases shown in Table 2, the model runs are more similar to each other than to the observations. The domain-wide temperature bias, computed as an average of the maximum and minimum temperature biases over all stations, is 0.69 degrees C for MM5 Test Run #1 and 0.47 degrees C for MM5 Test Run #2. The additional vertical resolution brings the average daily temperature bias within the proposed daily performance goal of 0.5 degrees C found in Table 1. However, substantially larger biases are present at certain times of the day and at certain stations. The predicted minimum temperatures are too high almost everywhere, with a maximum bias of 3.8 degrees C and 3.5 degrees C at Conroe for MM5 Test Run #1 and MM5 Test Run #2, respectively. The maximum temperatures show less bias, but the error tends to grow with time. Overall, the initial model runs are deficient in the amplitude of the diurnal cycle, underestimating the warming during the day and the cooling at night, especially during the latter half of the episode.

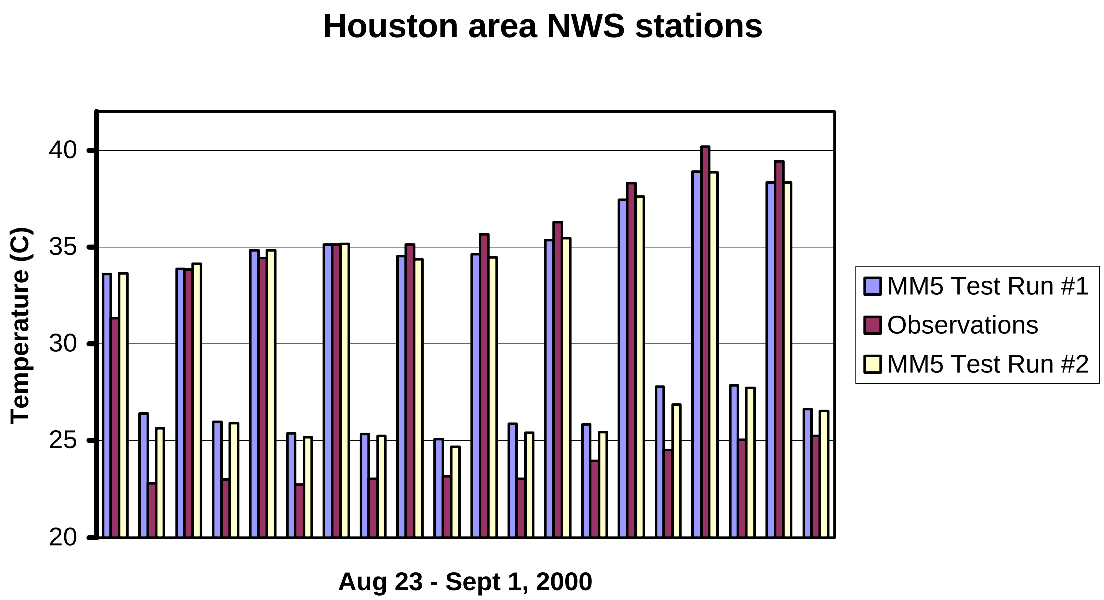

Figure 33. Comparison of hourly maximum and minimum temperatures averaged from eight station locations in the Houston area with two model forecasts. Successive groupings of data, from left to right, are maximum temperatures, August 23, 2000, minimum temperatures, August 24, maximum temperatures, August 24, etc. (Nielsen-Gammon, 2001).

Table 2. Average daily maximum and minimum temperature biases, 8/25/00 – 9/1/00

		MM5 Test Run #1	MM5 Test Run #1	MM5 Test Run #2	MM5 Test Run #2
Station	Station ID	Max bias Deg C	Min bias Deg C	Max bias Deg C	Min bias Deg C
Lake Jackson	LBX	-0.1	3.3	-0.1	2.8
Conroe	CXC	-1.4	3.8	-1.5	3.5
Hobby airport	HOU	0.8	1.9	0.9	1.5
Spring	DWH	-1.5	3.2	-1.4	2.9
Ellington Field	EFD	-0.5	2.6	-0.5	2.2
Bush Intercont	IAH	-1.5	2.8	-1.5	2.4
Galveston	GLS	0.4	0.7	0.3	0.8
Brenham	11R	-2.1	0.4	-2.1	0.0
Hou area avg		-0.7	2.4	-0.7	2.1
Coastal plain avg		-1.3	2.2	-1.3	1.8
Inland station avg		-2.0	3.1	-2.1	2.5

The poor minimum temperature forecasts would be expected to have little direct impact on ozone concentrations; however, the warm bias of minimum temperatures implies that the nighttime stratification might be too weak. During the daytime hours, solar heating generates a convective boundary layer from 1 to 3 km in depth that is generally well-mixed and characterized by relatively uniform winds. In general, MM5 is able to successfully simulate the daytime mixed layer. However, after sunset, the boundary layer becomes more complex as cooling of the land surface and the stable atmosphere contribute to the development of a shallow, near-surface layer that becomes decoupled from one or more overlying residual layers. These nocturnal residual layers are often characterized by very different physical properties and their development and evolution are not well simulated by meteorological models. In particular, MM5 has been unable to accurately simulate the decoupling of the shallow, near-surface layer such as that described during Regime II in key scientific question #1. This, in turn, can lead to nighttime surface wind speeds that are too high and nighttime winds aloft that are too weak, contributing to erroneously high nighttime mixing of chemical constituents and erroneous transport. The stronger nighttime winds could also negatively impact the subsequent evolution of winds during the day.

The transfer of heat between the land surface and atmosphere directly affects the PBL through turbulent transport. Given the drought conditions that dominated most of Texas during the late August and early September period, it was reasonable to modify the soil moisture to improve consistency with boundary layer temperature and moisture observations. Comparisons of model output to sounding data suggested that the model was predicting an overly moist boundary layer.

After a number of sensitivity runs, the soil moisture availabilities were adjusted to reflect the temporally varying conditions that occurred during the August 25 - September 1 period. Precipitation events that occurred in the Houston area during the four ramp-up days (August 22 – August 25) supported the use of the default (based on climatology and season) MM5 soil moisture availabilities. Given the very hot and dry conditions that persisted during the remainder of the period (August 26 – September 1), the soil moisture availability was decreased by up to 67 percent for most land use categories in the HG area, with the notable exception of urban areas. Lawn watering likely kept the urban soil relatively moist compared to that of the surrounding areas; therefore, urban soil moisture availability was actually increased compared to the default value throughout the episode.

Figure 34 compares the observed maximum and minimum temperatures to those predicted by the two MM5 test run simulations that utilized the modified soil moisture availabilities. MM5 Test Run #2 is similar to the runs presented in Figure 33, and has the same weak or nonexistent cool bias for maximum temperatures during the first few days of the episode. By the end of the episode, the cool bias exceeded 1 degree C. MM5 Test Run #3, which is similar to MM5 Test Run #2 but has even lower moisture availability, shows that that the maximum temperature bias is too warm by approximately 1 degree C after the first ramp up day but is essentially zero bias during the second half of the episode. Taken together, these runs demonstrate that the specification of varying soil moisture throughout the period results in an MM5 simulation that accurately predicts the maximum temperature observations. The best temperature forecast results are thus obtained by using the MM5 Test Run #2 configuration earlier in the episode and the MM5 Test Run #3 configuration later in the episode. Table 3 shows the recommended soil moisture characteristics for the optimal model run. The progressively drier soil moisture availabilities are consistent with the weather conditions that prevailed in Southeast Texas during the period.

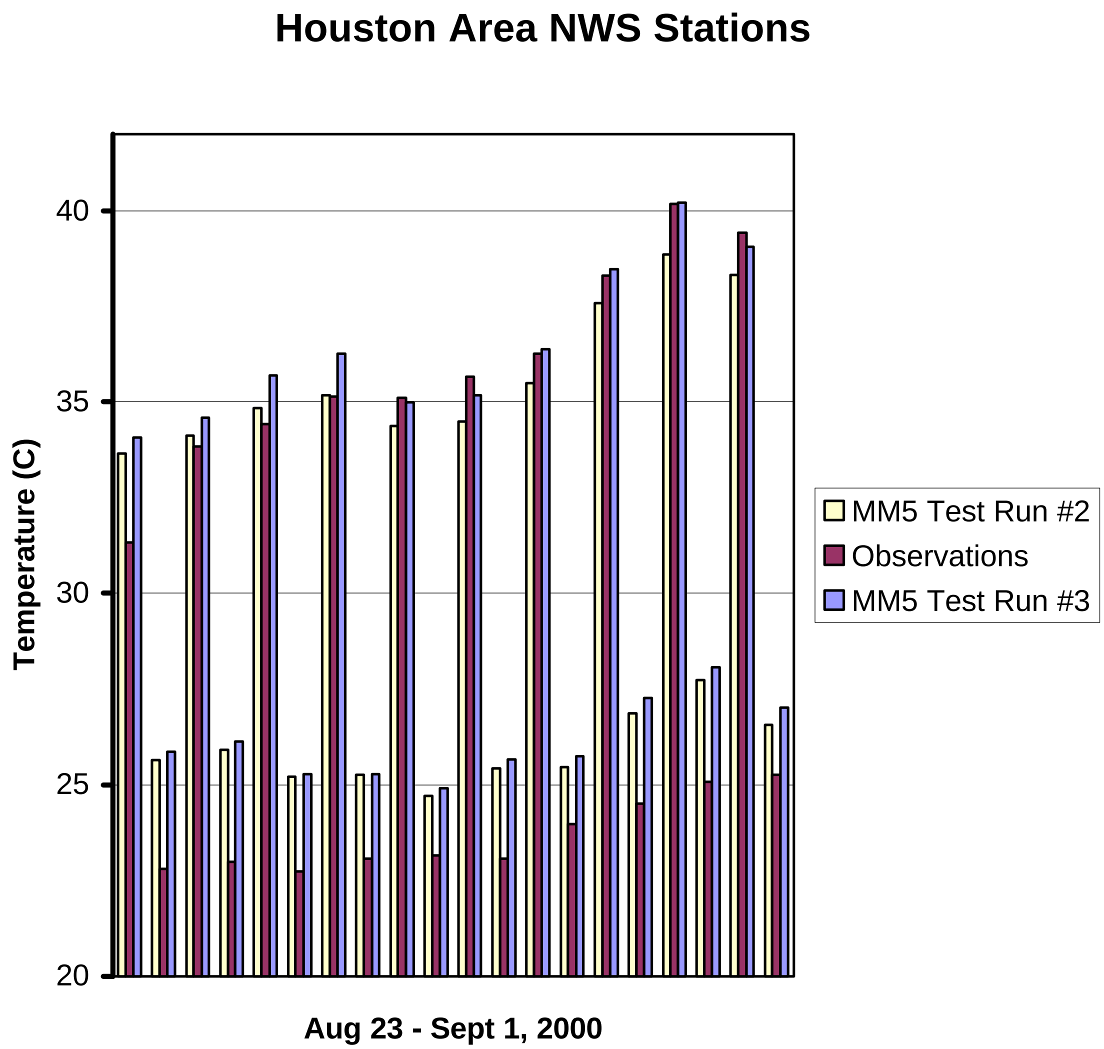

Figure 34:. Comparison of hourly maximum and minimum temperatures averaged from eight station locations in the Houston area with two model forecasts using reduced soil moisture availabilities. Successive groupings of data, from left to right, are maximum temperatures, August 23, 2000, minimum temperatures, August 24, maximum temperatures, August 24, etc. (Nielsen-Gammon, 2002a).

Table 3: Optimal MM5 soil moisture availabilities for the August 2000 episode by land use category.

Name	Category	108 km and 36 km grids	12 km grid	4 km, 00 UTC Aug. 22 to 00 UTC Aug. 26	4 km, 00 UTC Aug. 26 to 00 UTC Aug. 28	4 km, 00 UTC Aug. 28 to 12 UTC Sept. 2
Urban and built-up land	1	.10	.10	.30	.20	.20
Dryland cropland and pasture	2	.30	.20	.30	.20	.10
Cropland/grassland mosaic	5	.25	.15	.25	.15	.10
Grassland	7	.15	.10	.15	.10	.10
Deciduous broadleaf forest	11	.30	.30	.30	.25	.15
Evergreen needleleaf forest	14	.30	.20	.30	.20	.10

Additional analyses demonstrated that the models using reduced soil moisture availabilities forecasted the large-scale spatial temperature patterns well; however, the models were less successful at simulating the daily minimum temperatures and the strength of the nocturnal temperature inversions. The failure of the model simulations to accurately reproduce the strength of the nocturnal inversion is consistent with the warm bias in minimum temperatures. The nighttime surface layer simulated by the model is effectively too deep due to enhanced mixing with the overlying, relatively warmer air. This likely contributed to the failure of MM5 to produce a nighttime heat island as the near-surface layer in the surrounding areas did not sufficiently cool. In contrast, relatively lower daytime mixing heights predicted by the model likely contributed to a daytime heat island that was stronger than that observed. It is possible that continued judicious specification of the land surface characteristics may improve the simulation of the urban heat island.

This work on soil moisture is ongoing and should be continued. It is not always easy to pinpoint the source of model error. For example, research by Robert Zamora of NOAA/ETL implies that radiative model errors may be present in the current Dudhia parameterization schemes used to calculate the surface fluxes of longwave and shortwave radiation. Recent work has shown that the Dudia shortwave scheme was not properly simulating the absorption of solar radiation by aerosols and stratospheric ozone and was overestimating the amount of solar radiation reaching the surface under clear skies. This error would also be expected to contribute to a deeper and drier nighttime boundary layer. Fortunately, the robust dataset collected during TexAQS provides a wealth of observations to investigate the critical atmospheric phenomena in the HG area. In particular, the boundary flux measurements made by NOAA/ETL at the LaPorte site during the field phase of TexAQS could be used to intercompare the modeled fluxes of sensible and latent heat and radiation to that predicted by the MM5 model.

PBL Schemes and Surface/Upper-Level Winds

The radar wind profiler, lidar, and boundary flux data collected during TexAQS also offer an excellent opportunity to evaluate MM5's ability to simulate the three-dimensional structure and evolution of the low-level wind field. As discussed in key scientific question #1, the HG area is characterized by complex local-scale flow patterns that challenge the capabilities of any meteorological model to accurately simulate the winds at the surface and in the vertical. As previously discussed, the preferred correction for any model deficiencies will be obtained by altering the forcing of the physical processes that affect the predictions of temperature and wind. Correct modeling of the growth of the PBL is essential.

Several distinct planetary boundary layer (PBL) parameterization schemes are available in the MM5 model. All PBL schemes are strongly affected by the exchange of heat, moisture, and momentum between the land surface and the atmosphere. In general, the land surface characteristics (e.g., albedo, roughness length, soil moisture availability) are not directly measured but are specified as a function of season and land use. The current MM5 land surface characteristics could continue to be refined. Remotely sensed satellite data or airborne thermal imagery could be used to improve the accuracy of the current land use on a grid point basis. Additional land surface categories may be created to represent transitional land use types between the urban and agricultural categories that dominate in the HG area. In addition, although representative land surface characteristics used in MM5 in the HG area are not quantified, there are ample observations of the effect of the land surface characteristics and their variations. These observations are of the diurnal surface temperature cycle, vertical structure of the boundary layer, and sea breeze strength, structure and evolution. These land surface effects can be used to "tune" the land surface characteristics to allow the model to correctly predict features such as the diurnal temperature cycle and sea breeze cycle in a dynamically consistent, realistic way. Sensitivity studies combined with analysis of observational data could then be used to analyze the affects of any modifications to model characteristics and to evaluate model performance. Such a strategy would not be possible without the robust dataset collected during TexAQS.

A number of MM5 experiments were performed to systematically evaluate the performance of various PBL schemes and configurations. Particular emphasis was placed on the development of nighttime temperature inversions, daytime well-mixed layers, and the vertical structure of winds and temperatures associated with sea breezes. Experiments were focused on the performance of the Medium Range Forecast (MRF) PBL scheme using a variety of model run options; however, the Gayno-Seaman PBL scheme was tested as well.

Selected comparisons to sounding data from the three TexAQS sounding locations (Houston Southeast, Houston Downtown, and Wharton Power Plant) demonstrated that all schemes overestimated the daytime mixing heights. The subjective assessment of PBL heights based on daytime soundings at the Houston Southeast site were compared to the MRF PBL scheme's computed PBL height. The MRF consistently overpredicted the PBL height by about 30%. Overall, the performance was acceptable; however, care must be taken when determining vertical mixing characteristics for photochemical modeling so that strong vertical mixing does not result in the diffusion of ozone and its precursor compounds too rapidly upward out of the reported daytime MRF PBL.

The sea breeze and low-level jet are complex dynamic features of the atmospheric circulation and their prediction depends on the PBL parameterization as well as other factors. Observations of the sea breeze typically show a weak to moderate inversion overlaying the strongest onshore flow, with the return flow strongest just above the inversion. The Gayno-Seaman PBL scheme produced the most realistic vertical structure, but the simulated sea breeze inversion was too strong. In contrast, the MRF PBL scheme produced a sea breeze that was too weak, with atmospheric stability that gradually increased with height up to the capping inversion. Depending on how vertical mixing is handled in the photochemical model, ozone and its precursors may be prone to diffuse too rapidly upward out of the advancing sea breeze air if the MRF scheme is used. Since the MRF PBL scheme was ultimately chosen for modeling the August 23 – September 1 episode, testing and possible modification of MRF PBL schemes should continue if the vertical mixing proves to be a problem with photochemical modeling.

The MRF PBL schemes consistently predicted nighttime temperature inversions that underestimated the rate of temperature increase with height. During Regime 1, the five nighttime soundings indicated an average increase of temperature of 4 degrees C over a depth of about 20 mb. The PBL schemes did not replicate the strength of this feature and produced inversions that averaged between 0 and 1.2 degrees C. During Regime 2, the temperature structure was strongly affected by the nighttime low-level jet. In a typical observed sounding, a very shallow surface inversion was capped by a 20 mb thick well-mixed layer, the mixing presumably due to mechanical mixing caused by the strong wind shear beneath the jet. Above this neutral layer was a strong inversion, a deeper stable layer, and above 920 mb, very weak stratification. Model simulations failed to duplicate this complex vertical structure, often lacking both the surface inversion and the overlying neutral layer. The model PBL height was often too low, resulting in a nighttime low-level jet that was too close to the ground and far weaker than observed. This suggests that the current models will overestimate the amount of nighttime vertical mixing and may underestimate regional transport of ozone and its precursor compounds. Continued testing and possible modification of the processes affecting vertical mixing and transport in the PBL schemes may be necessary to improve the simulation of the low-level jet.

The MM5 model has several categories of land surface, including urban, agricultural, forest, and marsh. Apparently the variations in land use that the MM5 is missing (and/or inaccuracies in the classification of grid-point land use) cause a significant fraction of the errors in the simulation of local wind variations. *It is recommended that analyses be* *performed to confirm the accuracy of the current land use classification used by MM5. It may also be necessary to develop additional land surface categories (particularly within grid-cell regions characterized by transitional or highly spatially varying land use) that will allow the user to better approximate land use features in the model. This should be an area of ongoing research*.

Nielsen-Gammon noted that the local-scale inhomogeneities of the land surface implies that the "best" model configuration cannot be determined from a comparison with observed PBLs at only three sounding stations, particularly when one station was close to the coastline. A better approach is the examination of maximum and minimum surface temperatures, for which more observing stations are available. These results have been summarized previously, and the MRF PBL with reduced soil moisture availability performed best overall.

Clouds and Precipitation

Nielsen-Gammon noted that clouds during the TexAQS episode primarily consisted of fair weather cumulus that formed at the top of the PBL in the morning and dissipated in late afternoon. A subjective assessment of cloud cover in the HG area, based on model-simulated incoming shortwave radiation and visible satellite pictures, showed that none of the model simulations had the proper day-to-day variations in cloud cover. In addition, the MM5 simulations can not resolve the fair weather cumulus clouds on the 4-km grid, and the clouds produced by the model had too large a horizontal extent. Under such circumstances, the simulation with the fewest clouds is usually the best for use in photochemical modeling. For the HG area, the MRF PBL scheme generated the fewest clouds.

Daily precipitation was simulated remarkably successfully with the MRF PBL schemes; seven to eight days out of ten had no significant precipitation errors. The models were good at simulating the general location, coverage, and strength of shower activity, although the precise location and timing were often in error. Of course, individual rain showers did not closely resemble actual rain showers. Individual showers were predicted to be 10-20 km across, much larger than observed showers, and outflows associated with individual showers tended to be too large and too strong. It should be also be mentioned that few significant rain events occurred in the Houston area after August 24th.

Grid Resolution

Accurate simulation of the temporal and spatial scales of ozone concentrations in the HG area will likely require photochemical modeling at grid resolutions approaching 1 km or less (The reader is referred to the companion document *Accelerated Science Evaluation of Ozone Formation in the Houston-Galveston Area: Photochemical Air Quality Modeling)*. Continued refinement of the meteorological models has included a sophisticated set of parameterizations which allows the models to simulate intra-day atmospheric processes at grid resolutions approaching 1 km or less. These finer resolution grids are often used to help improve the model simulation of local-scale variability (e.g., the subtleties of the sea/bay breezes due to local variations of the land surface or the fine-scale structure of the sea breeze front).

As previously discussed in the section on historical modeling, the final meteorological fields produced by SAIMM for the 6-11 September 1993 episode exhibited a number of unrealistic features in the surface wind field that could not be explained from a physical perspective. TNRCC recently contracted with ENVIRON and MRC to replicate the 6-11 September 1993 episode using both RAMS and MM5 at a grid resolution of 1.33 km. Preliminary analyses of these runs included a qualitative comparison of the surface winds predicted by the RAMS model at a grid resolution of 1.33 km to those predicted at 4 km. The higher grid resolution presumably allowed the model to better respond to small-scale variability in the land surface, and a marked improvement in the detail of local-scale circulation features was observed. For example, Figure 35 presents the observed winds on 8 September at 1500 CST over the HG area. A well-developed sea breeze circulation is apparent in the observations, with onshore flow along the coast and light northeasterly flow over metropolitan Houston. The model run at a grid resolution of 4-km did a good job of simulating the observations, as shown in Figure 36. The sea breeze can be easily identified running parallel to the coast south of metropolitan Houston. Note, however, the striking increase in detail provided by the model run at 1.33 km, shown in Figure 37. The results on the higher resolution grid reveal the interaction of the Gulf and Bay breezes in far greater detail, and the flows over the Gulf are no longer smooth and uniform due to forcing from large-scale features. The relatively higher wind speeds over the bay (as expected, due to relatively lower surface roughness compared to the land surface) are clearly simulated, in addition to the sharp reduction in wind speed as the flow impacts the land. Also note the convergence over the Houston area caused by effects of the urban heat island combined with relatively greater surface roughness.

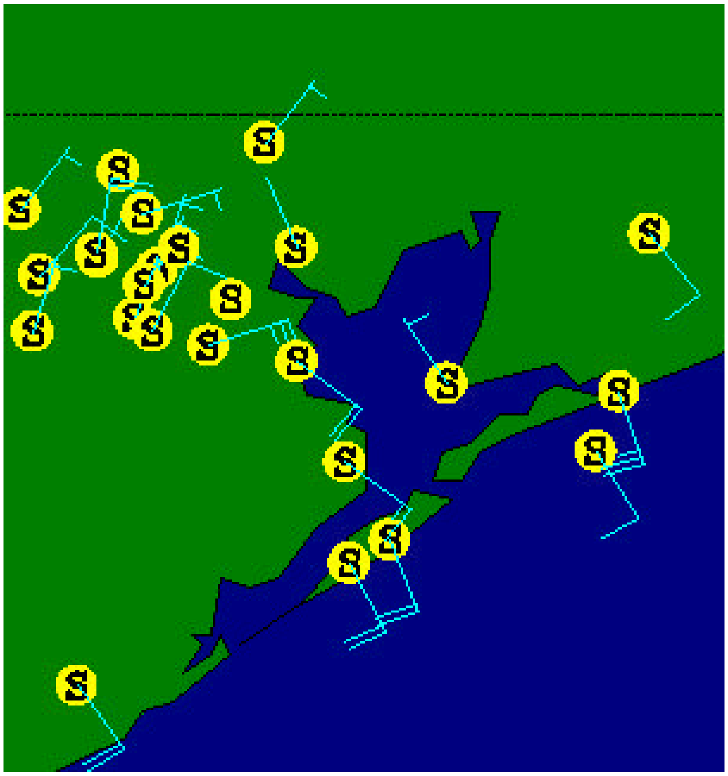

Figure 35: Observed surface wind field, September 8, 1993, 1500 CST.

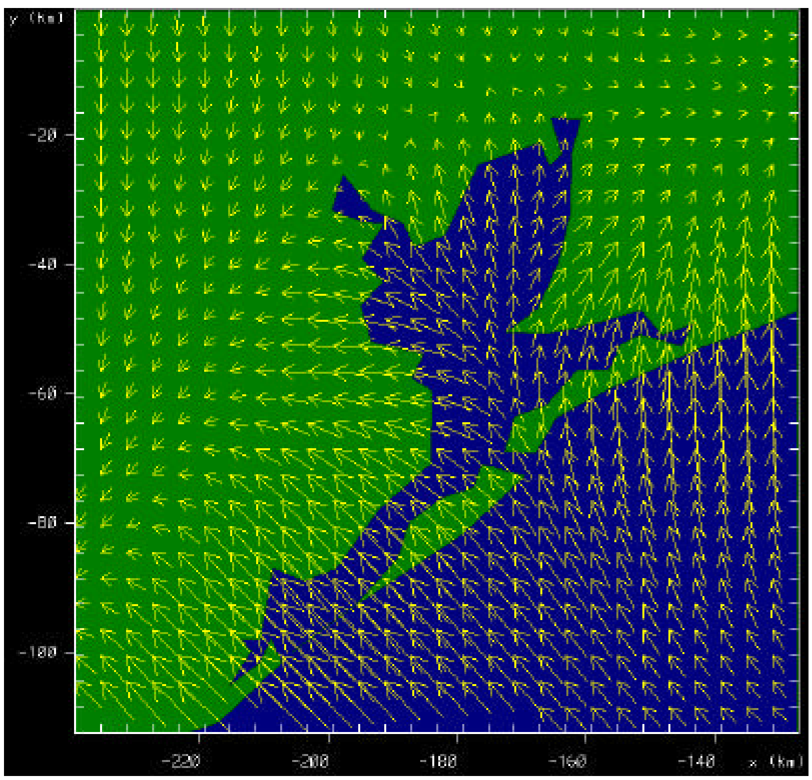

Figure 36: RAMS surface wind field on 4 km grid, September 8, 1993, 1500 CST.
Vectors are plotted at every grid point.

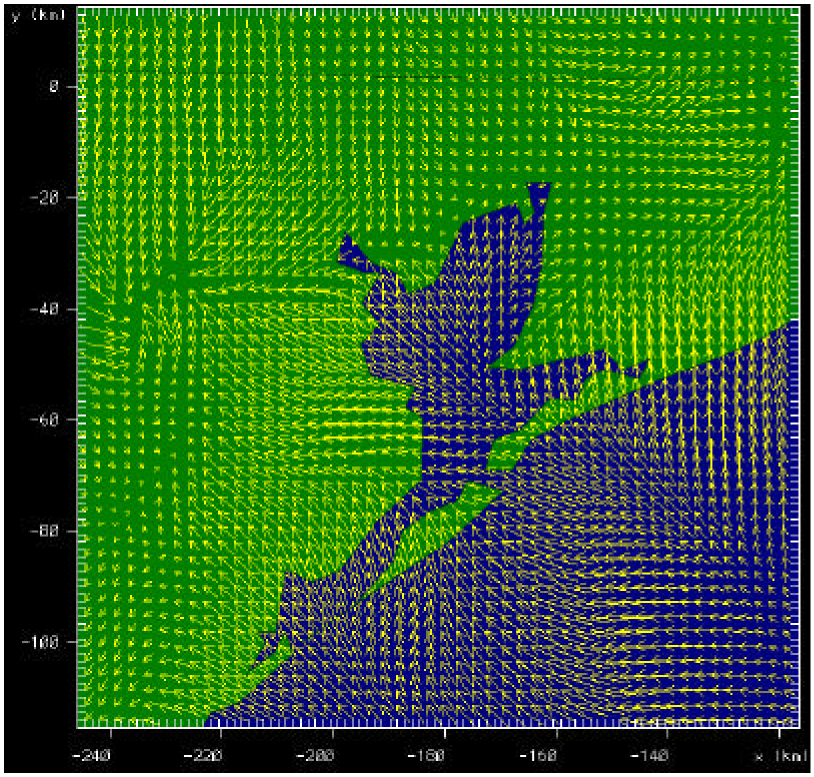

Figure 37: RAMS surface wind field on 1.33 km grid, September 8, 1993, 1500 CST. Vectors are plotted at every grid point.

There are a number of issues to consider when decreasing the horizontal grid size of meteorological models to 1 km or less. First, many aspects of model performance will not be improved if the required inputs (e.g. land use, soil moisture, albedo, etc.) are not accurately resolved to the grid spatial scale. Second, the time and space scales of atmospheric processes may require reductions in the temporal resolution of meteorological (e.g., reduce current one-hour interval for meteorological output) and photochemical model (e.g., reduce averaging time for emission rates) inputs. Finally, the sub-grid parameterizations used by the current generation of meteorological models must be carefully examined to avoid "double counting" the energy of smaller-scale atmospheric processes that are resolved by the increased horizontal resolution. For example, preliminary modeling of the HG area performed by R. Zamora indicated that the sensitivity of the model to land use boundaries increases as the grid spacing shrinks. Such results demonstrate that the meteorological model must be carefully examined to determine if the model is capable of simulating atmospheric processes at the desired grid resolution. Sensitivity analyses should be developed to test and, if necessary, refine the model parameterizations for use with small horizontal grids.

Overall model performance is not necessarily improved by using a finer grid resolution. Even if the increased grid resolution enables the model to resolve small-scale features such as turbulent eddies, accurate prediction of the time, place, and depth of these features is unlikely. Grid-based models will always be limited not only by the necessary parameterizations of sub-grid processes, but also by imperfect formulation of model physics and random and systematic errors in the input data. The impact of these errors increases as the horizontal grid size decreases. Careful evaluation of the advantages and disadvantages of increased horizontal grid resolution must be considered before committing to a finer resolution grid.

4. How can observations best be assimilated into a meteorological model to enhance its representation of these processes?

As indicated in the discussion in key scientific question #3, there are two basic ways to utilize observed meteorological data in running MM5. The best approach is to adjust model parameterizations so that the model will correctly simulate all atmospheric processes. This approach is rarely completely successful, due to limitations in the parameterizations, knowledge of the physical processes in the atmosphere, or error growth from chaotic atmospheric dynamics. The second is to assimilate the data into the model directly. This process is generally called four-dimensional data assimilation (FDDA); the specific implementation of this technique in the MM5 model (and many other models) is called nudging. As described earlier in this report, strong nudging of surface winds from SAIMM caused discontinuities in the meteorological fields in the September 1993 episode. In this case, the agreement with observations may have been improved, but the model performance at areas without observations was likely degraded.

Most meteorological models can take advantage of (1) analysis nudging and (2) observational nudging. Analysis nudging uses gridded analyses of winds, temperature, and humidity, typically from the analysis cycle of an operational forecast model such as those operated by the National Weather Service (NWS). Such a dataset is also used to supply the initial and boundary conditions required for the meteorological model, whether or not analysis nudging is to be employed. The NWS analyses include data obtained from a combination of observation systems, including routine surface, upper air, radar, and satellite observations.

Observational (or point) nudging is used to nudge the meteorological model toward measurement data at individual sites within the specific region of interest. For example, previous meteorological modeling for the 8-county HG ozone nonattainment area has used routinely collected wind speed, wind direction, relative humidity, and temperature data measured at approximately 25 (the exact number varies from year to year) continuous monitoring stations. Upper air observations of wind speed, wind direction, and temperature collected from twice daily rawinsonde soundings and limited wind radar profiler and sodar sounders were sometimes used as well. (It should be noted that previous modeling in the HG area has been hampered by lack of local data; profiler data were unreliable and the nearest rawinsonde soundings were taken at Lake Charles and Corpus Christi.)

Observational Nudging of the Winds

Sea breeze formation and inland penetraton is very sensitive to the speed and direction of the large-scale winds (Nielsen-Gammon, 2001, 2002a, 2002b). FDDA can be used to nudge one or more of the modeled grids to the same synoptic scale wind analyses used to prepare the initial and boundary conditions. However, the frequency and strength of the FDDA analysis nudging must be studied carefully to avoid detrimentally affecting the intra-day and diurnal wind cycles. Sensitivity modeling must often be performed to determine the optimal frequency of nudging and the specific grid or grids to nudge. Nielsen-Gammon has experimented with various approaches for analysis nudging of MM5 results in the HG area. His results indicate that when analysis nudging with the EDAS data was applied to the 108 km, 36 km, and 12 km grid cells, the model predicted better large-scale winds than if the nudging was not performed on the smaller 12 km grid cells. (Nielsen-Gammon, 2001).

Observational nudging should be used with caution. As shown in many of the SIP modeling results discussed earlier in this document, strong FDDA observational nudging can lead to unrealistic responses in the model. The preferred method before applying FDDA is to use the observations to refine the model characteristics so that the model accurately simulates the particular atmospheric process, as discussed in key scientific question #2. For example, consider a model forecast of a sea breeze front in which the simulated front moves inland too slowly. This deficiency in the model may be due to a number of factors, such as an overly strong large-scale wind over land. The preferred technique for correcting this problem would be to identify the cause of the wind speed error (for example, an incorrect analysis being assimilated on the large-scale grid) and correct it.

Unfortunately, modeling performed by Nielsen-Gammon using only analysis nudging resulted in wind speed errors that were too high when compared to the performance goals shown in Table 1. Comparisons to data obtained from the five TexAQS radar wind profilers were used to compute wind errors at a variety of heights, grouped by weather Regime, using 24-hour running means and departures from running means. The wind directions are analyzed in terms of the u (east-west) components and the v (north-south) components. Figure 38 shows the RMS error of the MM5 Test Run #2 at 200 m, 400 m, 700 m, and 1000 m. Note that the RMS errors at all heights exceed the performance goal of 1.4 m/s (1.4 m/s is the east-west and north-south component of the overall 2 m/s performance goal). The plots include overall RMS errors as well as RMS errors in the 24-hour running mean and RMS errors of the departures from the running mean. All three types of RMS errors tend to be largest at 400 m, where the sea breeze and low-level jet are both strong. The RMS errors of the departure from a running mean account for most of the overall RMS error at all levels, indicating that the winds are dominated by phenomena with periods of 24 hours or less.

Figure 39 presents the model biases. The model wind components greatly exceeded the total wind speed performance goal of +/-0.5 m/s at most heights. The model developed large biases at heights above 1 km. There is an increasing model bias in the u component with height. According to thermal wind laws, this model bias may be associated with erroneously cool temperatures in the models between 1000 m and 3000 m.

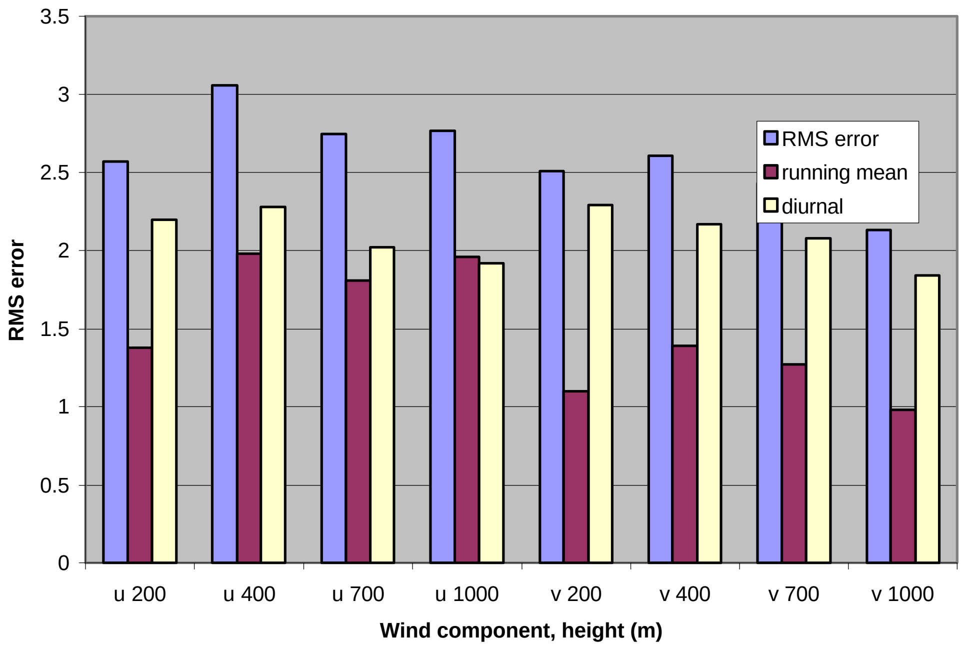

Figure 38: Total RMS error, RMS error of the 24-hour running mean, and RMS error of the departure from the 24-hour running mean, by wind component and height above ground (m), MM5 Test Run #2. U represents the east-west wind direction component and v represents the north-south wind direction component.

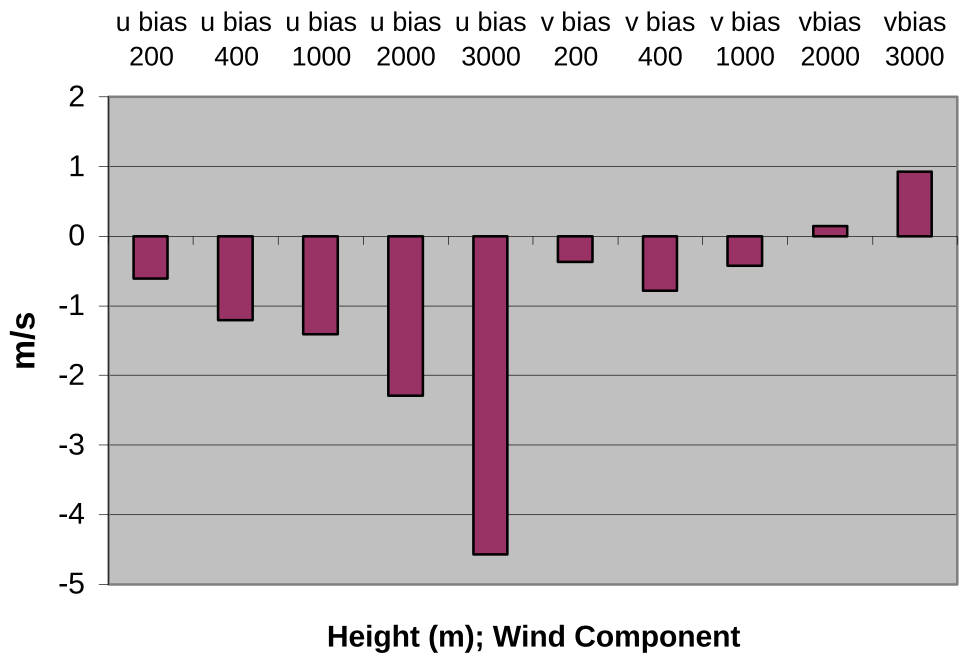

Figure 39: Bias as a function of wind component and height (m) measured against ETL quality-controlled profiler data, MM5 Test Run #2.

Measurements from the TexAQS profiler network provided an excellent source for data assimilation. By careful selection of the temporal averaging period, the small-scale wind variations could be effectively separated from the larger-scale flow. Analysis of the profiler data demonstrated that the diurnal wind cycle is a large-scale dynamic response that is seen in all five profilers. It was important to select an averaging period for the nudging analysis that effectively smoothed out local, small-scale circulations without losing too much information on the diurnal (24-hour) cycle. After careful consideration, an averaging period of 4 hours was selected for the observational nudging. This averaging period, combined with the distance between the profiler stations, inherently suggested a nudging radius of influence (spatial scale) of approximately 150 km.

Figure 40 shows the RMS error for the two wind components at various heights for the model runs using observation nudging to the profiler data. (It should be mentioned that any statistics based on comparisons between the profiler and model data will overestimate the degree of improvement caused by nudging. To evaluate the performance objectively, a portion of the profiler data should be withheld from the FDDA and used only to evaluate model performance.) By standard statistical measures, the wind field above the ground at the profiler sites is tremendously improved. The overall RMS errors are between 1.3 and 1.8 m/s and improve with height. The improvement is largest in the running 24-hour mean, where typical RMS errors have decreased by more than a factor of two.

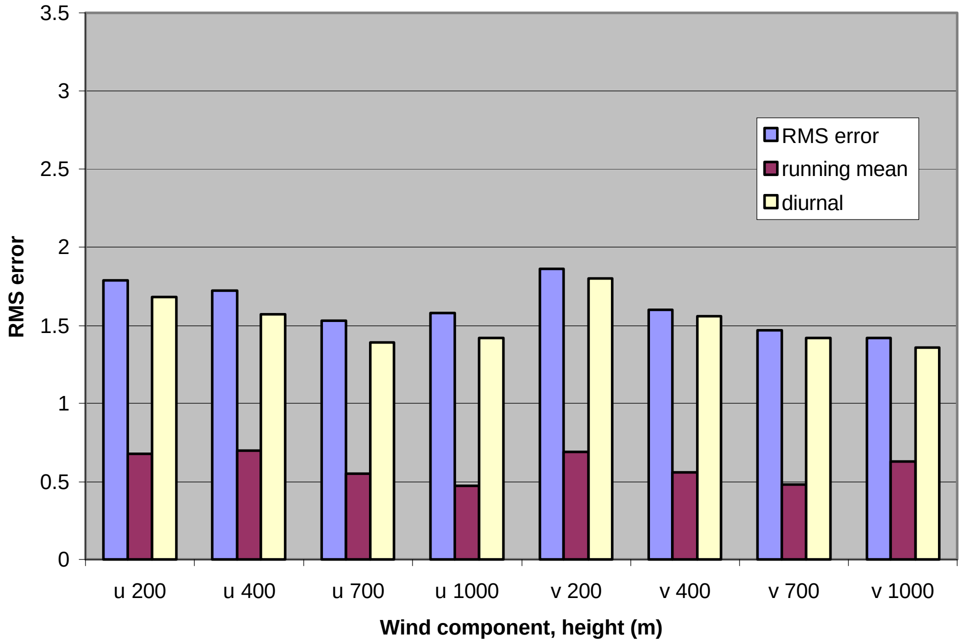

Figure 40: Total RMS error, RMS error of the 24-hour running mean, and RMS error of the departure from the 24-hour running mean, by wind component and height above ground, driver model run. Compare with Fig. 35.

As shown in Figure 41, the model biases with observational nudging to the profiler data also show tremendous improvement. Most biases are less than 0.3 m/s below 2500 m, well below the performance goal of +/-0.5 m/s. Even at 3000 m, where profiler data is more sparse, the biases are reduced by nearly a factor of two. Based on the improvement in the running mean RMS and overall bias, it appears that the observational nudging has accomplished its primary goal of correcting the large-scale, slowly-varying wind field. In the diurnal component, or departures from the 24-hour running mean, the improvement is greatest during Regime 2. RMS errors in Regime 2 have decreased by a factor of two with the observational nudging. Regime 1 improvements are smaller, but the statistical model performance in Regime 1 is better than that for Regime 2.

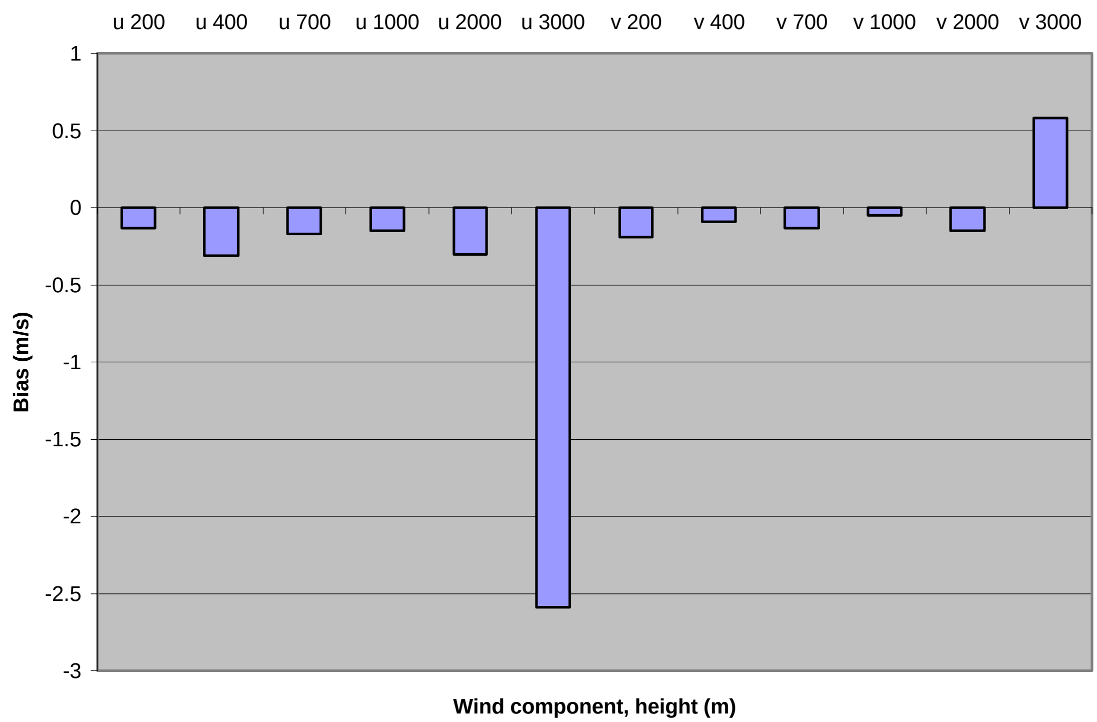

Figure 41: Bias as a function of wind component and height, driver model run. Compare with Fig. 36.

Assimilation of Satellite Data

It may be important to consider the assimilation of satellite-derived data (particularly cloud cover and soil moisture) into the FDDA datasets as well. For example, current meteorological models simulate clouds in a highly parameterized manner and are unable to effectively predict their spatial and temporal distributions. Nielsen-Gammon noted that clouds during the TexAQS episode primarily consisted of fair weather cumulus. The scale of these clouds is smaller than the 4 km simulations can represent, and neither the shallow cumulus parameterization nor the boundary-layer parameterizations used in the model runs include a parameterization of solar radiation blockage by sub-grid scale boundary-layer cumulus.

When such clouds are incorporated into a photochemical model simulation, significant uncertainty in predictions of surface insolation and temperature are introduced, which could result in erroneous predictions of ozone in the photochemical model. If this proves to be a problem during the photochemical modeling, it may be advantageous to specify the incoming radiation from observational data rather than use the radiation computed by the meteorological model.

Algorithms have been developed that adjust the calculation of meteorological variables by incorporating the satellite-derived location and spatial extent of clouds (Lapenta et al,, 2000). Similarly, algorithms are being developed to adjust model soil moisture using satellite-sensed skin temperatures (McNider, 2001). Since soil moisture is rarely measured, this technique will provide a powerful tool to improve upon the default values assumed based on the limited data set used for land type and season. Satellite data can also be used to provide other types of information needed by the meteorological models, such as albedo and land use. Where possible, the assimilation of satellite data should be fully exploited for the TexAQS meteorological model runs.

5. What is the minimum set of routine observations needed to adequately simulate the meteorological parameters used for photochemical grid modeling?

After a modeling approach has been defined so that the meteorological and photochemical models can accurately predict meteorological observations, then the fifth key scientific question must be addressed: What is the minimum set of routine observations needed to adequately simulate the meteorological parameters used for photochemical grid modeling? Since this set of observations will be used by TNRCC to review the monitoring network in the HG area, the location and frequency of observations should be carefully evaluated for each measurement type. The most desirable situation would be to routinely collect a sufficient set of observations that could be used to simulate the complex meteorology in the area with meteorological models instead of having to rely upon data collected during intense field studies. This would enable TNRCC to accurately model any set of conditions that are correlated with high ozone, rather than being restricted to modeling only those conditions that occurred during an intensive field study.

After the MM5 parameterizations have been adjusted to obtain adequate model performance, the model results should be carefully analyzed to determine if there are locations where the model predicts significant meteorological phenomena that can not be verified by the routine observations. This analysis should be performed in conjunction with the photochemical grid model performance. For example, the meteorological and photochemical modeling results for the September 1993 episode predicted a localized region of elevated ozone concentrations near the Croquet monitoring site on September 8. Using the results of two other meteorological models to drive the photochemical model produced basically the same feature; however, the Croquet monitor measured significantly lower ozone than predicted by these runs. Given the spacing of monitors in the region, it is not possible to determine if 1) the air parcel containing high ozone concentrations did develop, but errors in the modeled winds transported the parcel over a different area or 2) the high ozone concentrations are an artifact of the models. If photochemical modeling using the meteorological data collected during TexAQS continues to predict similar events, it may be important to locate additional surface monitors in strategic areas.

The enhanced observational network employed during TexAQS included six radar wind profilers and additional rawinsonde sounding sites. These data provide detailed information on the vertical structure of the atmosphere, and are being utilized for model performance evaluation and analysis nudging of the 12 km and larger grids. Sensitivity testing should be performed to determine the minimum number of radar profilers and rawinsonde sounding sites needed to provide sufficient data to obtain good MM5 model performance. In particular, parallel simulations and model evaluations should be conducted with and without the special TexAQS data.

Modeling of historical episodes such as those from 1998 and 1999 could also be used to help determine if the routine data collection network is adequate to provide data for model performance evaluation and analysis nudging. These new historical episodes could be modeled using the refined MM5 parameterizations developed for the TexAQS episode**.** The MM5 model performance would be evaluated based on the available data to determine if this routine data set is adequate to measure model performance.

6. Are linkages between meteorological and photochemical grid models accurately transferring wind field information?

The results from the meteorological model are used as inputs to the photochemical grid model. This leads to the sixth key science question, which relates to the transfer of information between these two models. Prognostic meteorological models are frequently run with a large number (41 or more) of vertical layers. To minimize computation time, the photochemical grid models are normally run with significantly fewer (8 to 12) vertical layers that are cut off at much lower levels in the atmosphere than the meteorological model layers. Normally the vertical structure of the photochemical grid model is designed so that the lowest layers are identical to the lowest layers used in the meteorological model. Usually the vertical structures are identical up to the height that is typical for the top of the mixed layer. For some of the upper layers of the photochemical grid model the meteorological data must be vertically averaged for input to the photochemical model. Sensitivity studies should be performed to determine the most appropriate vertical structure to use for the photochemical grid modeling. This would include sensitivity testing to determine the number of vertical layers needed in the photochemical grid model to obtain adequate photochemical grid model performance. The number of preferred vertical levels may be region specific. For example, the vertical grid structure needed in the HG area may be different than that needed in the Dallas area.

For its calculations, MM5 does not conserve mass. However, the photochemical grid models require that mass is conserved to perform their calculations. The photochemical model takes the data from the meteorological model and processes it so that the meteorological fields used in the photochemical modeling will conserve mass. During this process vertical velocities may be artificially modified for the photochemical modeling. This can occur even if the vertical structures of the two models are identical. If unrealistic vertical velocities are calculated by the photochemical model, it will be necessary to reevaluate the vertical structures of the meteorological and photochemical models to determine a better vertical structure for both models. By nature this process is iterative.

Summary

The preliminary meteorological modeling done for the TexAQS period suggests that the meteorology correlated to formation of high ozone is more complex than previously thought. These findings will be used to revise the conceptual model for formation of high ozone in the HG area.

Further, the preliminary modeling indicates that land surface characteristics, model vertical grid structure, and the algorithm used for parameterization of the planetary boundary layer will be among the more sensitive inputs for meteorological models. Along with model improvement, activities underway are use of satellite data to refine the surface characteristics used in the meteorological model to simulate heating cycles and the assimilation of upper air wind measurements to fine tune meteorological model performance. Also underway are testing activities to determine the best approaches for meteorological model run options related to vertical structure and algorithms to characterize planetary boundary layer physics.

References

"Accelerated Science Evaluation of Ozone Formation in the Houston-Galveston Area: Atmospheric Chemistry", 2001.

"Accelerated Science Evaluation of Ozone Formation in the Houston-Galveston Area: Emissions Inventory", 2001.

Arritt, R. W. 1985, "Numerical Studies of Thermally and Mechanically Forces Circulations Over Complex Terrain", Cooperative Institute for Research in the Atmosphere, Colorado State University, Fort Collins, Colorado.

ENVIRON, 2001 -Environ International Corporation, "MM5/RAMS Fine Grid Meteorological Modeling for September 8-11, 1993 Ozone Episode", August 2001.

ENVIRON, 2001a - Environ International Corporation, "Enhanced Meteorological Modeling and Performance Evaluation for Two Texas ozone Episodes", August, 2001.

Federal Clean Air Act Amendments of 1990 (42 United States Code (USC))

Kessler, R. "Users Guide-System Applications, Inc. Versions of the Colorado State University Mesoscale Model (Version 2), Systems Applications International, 1989.

Kessler, R, Douglas, S, "User's Guide to the Systems Applications. International Mesoscale Model", Systems Applications International, 1993.

Lapenta, W, et al, "Operational Assimilation of GOES Data into a Mesosale Model", 10th Conference on satellite Meteorology and Oceanography, 2000.

McDonald-Buller, E.C., et al, "Impacts of Regional Control strategies on Air Quality in Eastern and Central Texas: Zeroing Out Emissions in Each of the Non-attainment and Near Non-attainment Regions", 2000.

Mahrer, Y and R. A. Pielke. 1977 "Diurnal boundary-layer development over sloping terrain." J. Atmos Sci, 38:2198-2212

Mahrer, Y. and R. A. Pielke. 1978 "A test of an upstream spline interpolation technique for the adjective terms in a numerical mesoscale model", Mon. Wea Rev., 106:818-830.

McNider, R, presentation at TexAQS Workshop, TNRCC, Nov 2001.

Minerals Management Service (1995), "Gulf of Mexico Air Quality Study, Final Report, MMS 95-0038, August, 1995.

Nielsen-Gammon, J.W., "Initial Modeling of the August 2000 Houston-Galveston Ozone Episode", Dec 2001.

Nielsen-Gammon, J.W., 2002a: “Evaluation and Comparison of Preliminary Meteorological Modeling for the August 2000 Houston-Galveston Ozone Episode”, Feb. 2002.

Nielsen-Gammon, J.W., 2002b: “Meteorological Modeling for the August 2000 Houston-Galveston Ozone Episode: PBL Characteristics, Nudging Procedure, and Performance Evaluation”, Feb. 2002.

Nielsen-Gammon, J., and S. Naumann. 2000 “Application of the MM5 Mesoscale Model to the Houston-Galveston Metropolitan Area”, July 2000.

Rotunno, R., 1983: “On the Linear Theory of the Land and Sea Breeze”, *Journal of the Atmospheric Sciences*, Vol. 40, pp. 1999-2009.

Senff et al., 2001. Presentation at TexAQS Data Workshop, University of Texas, August 2001.

Texas Natural Resource Conservation Commission (1994), “Attainment Demonstration for the Houston/Galveston Ozone Nonattainment Area”, Nov 1994.

Texas Natural Resource Conservation Commission, “Air Quality Modeling Guidelines – RG-025-Revised- February 1999”, Feb 1999

Texas Natural Resource Conservation Commission, “Attainment Demonstration for the Houston/Galveston Ozone Nonattainment Area, Appendix B, Base Case Emissions Inventory”, Feb 20, 1998.

Texas Natural Resource Conservation Commission, “Post-1999 Rate-of-Progress and Attainment Demonstration SIP for the Houston/Galveston Ozone Nonattainment Area”, Dec 6, 2000. Available at www.tnrcc.tx.us/oprd/sips.

Texas Natural Resource Conservation Commission, “Conceptual Model for Ozone Formation in the Houston-Galveston Area”, 2001.

U. S. Environmental Protection Agency (1981) “Guidelines for Use of City-Specific EKMA in Preparing Ozone SIPs”, EPA-450/4-80-027, 1981

U. S. Environmental Protection Agency (1986) “Guideline on Air Quality Models (Revised), EPA-450/2-78-027R, July 1986.

U. S. Environmental Protection Agency (1991) “Guideline for Regulatory Application of the Urban Airshed Model”, EPA-450/4-91-013, July 1991.

Appendix A

This appendix is an excerpt from the ENVIRON report that addressed meteorological model performance evaluation (ENVIRON, 2001).

The statistical measures listed in the section on performance evaluation can be more explicitly defined as shown below from information taken directly from the ENVIRON report.

Mean Observation (M_o): calculated from all sites with valid data within a given analysis region and for a given time period (hourly or daily):

$$M_o = \frac{1}{IJ}\sum_{j=1}^{J}\sum_{i=1}^{I} O_j^i$$

where O^i_j is the individual observed quantity at site i and time j, and the summations are over all sites (I) and over time periods (J).

Mean Prediction (M_p): calculated from simulation results that are interpolated to each observation used to calculate the mean observation (hourly or daily):

$$M_p = \frac{1}{IJ}\sum_{j=1}^{J}\sum_{i=1}^{I} P_j^i$$

where P^i_j is the individual predicted quantity at site i and time j. Note that mean observed and predicted winds are vector-averaged (for east-west component u and north-south component v), from which the mean wind speed and mean resultant direction are derived.

Least Square Regression: performed to fit the prediction set to a linear model that describes the observation set for all sites with valid data within a given analysis region and for a given time period (daily or episode). The y-intercept a and slope b of the resulting straight line fit are calculated to describe the regressed prediction for each observation:

$$\hat{P}_j^i = a + bO_j^i$$

The goal is for a 1:1 slope and a "0" y-intercept (no net bias over the entire range of observations), and a regression coefficient of 1 (a perfect regression). The slope and intercept facilitate the calculation of several error and skill statistics described below.

Bias Error (B): calculated as the mean difference in prediction-observation pairings with valid data within a given analysis region and for a given time period (hourly or daily):

$$B = \frac{1}{IJ}\sum_{j=1}^{J}\sum_{i=1}^{I}\left(P_j^i - O_j^i\right)$$

Gross Error (E): calculated as the mean *absolute* difference in prediction-observation pairings with valid data within a given analysis region and for a given time period

$$E = \frac{1}{IJ}\sum_{j=1}^{J}\sum_{i=1}^{I}\left|P_j^i - O_j^i\right|$$

(hourly or daily).

Note that the bias and gross error for winds are calculated from the predicted-observed residuals in speed and direction (not from vector components *u* and *v*). The direction error for a given prediction-observation pairing is limited to range from 0 to ±180°.

Root Mean Square Error (RMSE): calculated as the square root of the mean squared difference in prediction-observation pairings with valid data within a given analysis region and for a given time period (hourly or daily):

$$RMSE = \left[\frac{1}{IJ}\sum_{j=1}^{J}\sum_{i=1}^{I}\left(P_j^i - O_j^i\right)^2\right]^{1/2}$$

The RMSE, as with the gross error, is a good overall measure of model performance. However, since large errors are weighted heavily (due to squaring), large errors in a small subregion may produce a large RMSE even though the errors may be small and quite acceptable elsewhere.

Systematic Root Mean Square Error ($RMSE_S$): calculated as the square root of the mean squared difference in *regressed* prediction-observation pairings within a given analysis region and for a given time period (hourly or daily):

$$RMSE_S = \left[\frac{1}{IJ}\sum_{j=1}^{J}\sum_{i=1}^{I}\left(\hat{P}_j^i - O_j^i\right)^2\right]^{1/2}$$

where the regressed prediction is estimated for each observation from the least square fit described above. The $RMSE_S$ estimates the model's linear (or systematic) error; hence, the better the regression between predictions and observations, the smaller the systematic error.

Unsystematic Root Mean Square Error ($RMSE_U$): calculated as the square root of the mean squared difference in prediction-regressed prediction pairings within a given analysis region and for a given time period (hourly or daily):

$$RMSE_U = \left[\frac{1}{IJ} \sum_{j=1}^{J} \sum_{i=1}^{I} \left(P_j^i - \hat{P}_j^i \right)^2 \right]^{1/2}$$

The unsystematic difference is a measure of how much of the discrepancy between estimates and observations is due to random processes or influences outside the legitimate range of the model.

A "good" model will provide low values of the RMSE, explaining most of the variation in the observations. The systematic error should approach zero and the unsystematic error should approach RMSE since:

$$RMSE^2 = RMSE_S^2 + RMSE_U^2$$

It is important that RMSE, $RMSE_S$, and $RMSE_U$ are all analyzed. For example, if only RMSE is estimated (and it appears acceptable) it could consist largely of the systematic component. This error might be removed through improvements in the model inputs or use of more appropriate options, thereby reducing the error transferred to the photochemical model. On the other hand, if the RMSE consists largely of the unsystematic component, this indicates that further error reduction may require model refinement (new algorithms, higher resolution grids, etc.), or that the phenomena to be replicated cannot be fully addressed by the model. It also provides error bars that may be used with the inputs in subsequent sensitivity analyses.

Index of Agreement (IOA): calculated following the approach of Willmont (1981). This metric condenses all the differences between model estimates and observations within a given analysis region and for a given time period (hourly and daily) into one statistical quantity. It is the ratio of the total RMSE to the sum of two differences – between each prediction and the observed mean, and each observation and the observed mean:

$$IOA = 1 - \left[\frac{IJ \cdot RMSE^2}{\sum_{j=1}^{J} \sum_{i=1}^{I} \left| P_j^i - M_o \right| + \left| O_j^i - M_o \right|} \right]$$

Viewed from another perspective, the index of agreement is a measure of the match between the departure of each prediction from the observed mean and the departure of each observation from the observed mean. Thus, the correspondence between predicted and observed values across the domain at a given time may be quantified in a single metric and displayed as a time series. The index of agreement has a theoretical range of 0 to 1, the latter score suggesting perfect agreement.